Review of magnetic and gravity fields accompanying volcanic and seismic activity

Ciro Del Negro, Gilda Currenti, Rosalba Napoli

Istituto Nazionale di Geofisica e Vulcanologia, Sezione di Catania

26-28 April 2010 – L'Aquila

Sezione di Catania

Istituto Nazionale di Geofisica e Vulcanologia

Permanent Magnetic Monitoring Networks

JOURNAL OF GEOPHYSICAL RESEARCH VOL. 74, NO. 27, DECEMBER 15, 1969

Volcano-Magnetic Effect Observed on Mt. Ruapehu, New Zealand

M. J. S. JOHNSTON AND F. D. STACEY

Department of Physics, University of Queensland, Brisbane 4067, Australia

Amplitude of Detected Magnetic Anomaly

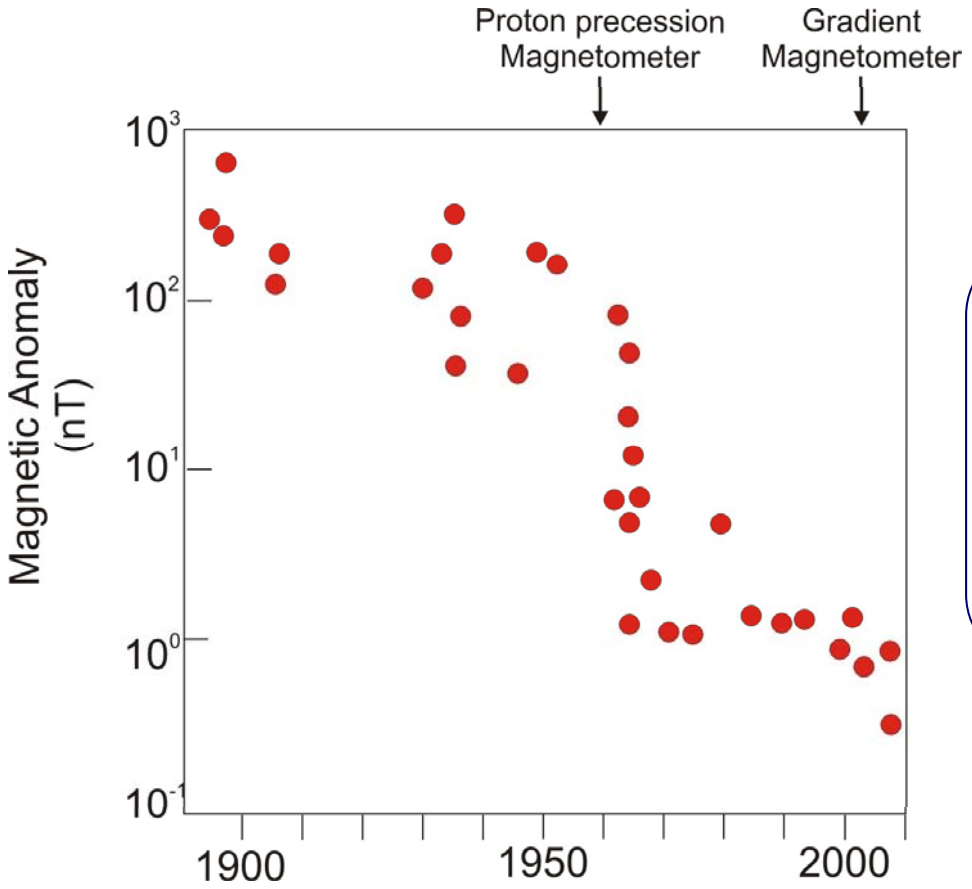

Plot shows decrease in observed magnetic anomalies with time. A significant decrease is related to the development of more accurate and stable instruments (updated from Rikitake, 1979; Muller and Johnston 1998).

Expected magnetic variation

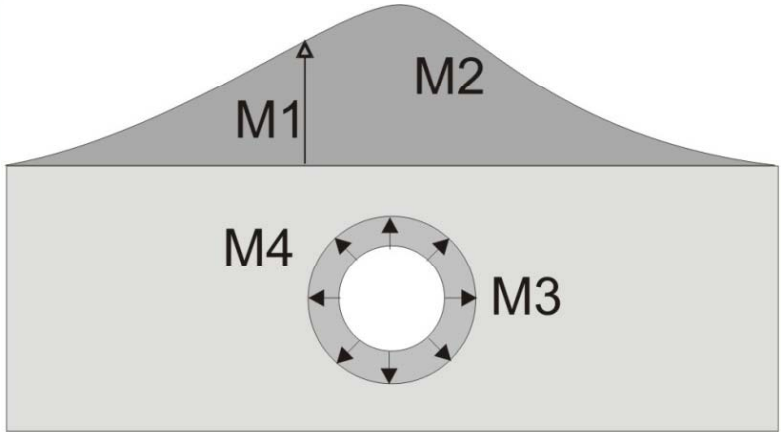

Magnetic variations can be accounted for by four contributions:
(M1) “free air” magnetic effect resulting from movement of the observation site in the Earth’s main field, (M2) the redistribution of magnetized mass, (M3) thermal demagnetization and remagnetization effect, (M4) change due to the piezomagnetic mechanism.

Piezomagnetism relates a rock’s magnetic properties to an applied stress and thus is a stress-dependent geophysical property that offers a potentially effective method for stress determination.

|M3| >|M4| >> |M2| >> |M1| (Sasai, 1991)

There are distinct differences in the geomagnetic distribution patterns resulting from piezomagnetism induced by an inflated pressure source and the thermal magnetic effects caused by spherical demagnetization. **Amplitude**, **time-scale**, and **polarity** of the volcanomagnetic anomaly allow to distinguish among them.

Sezione di Catania

Unrest

Rest

Piezomagnetic Effect

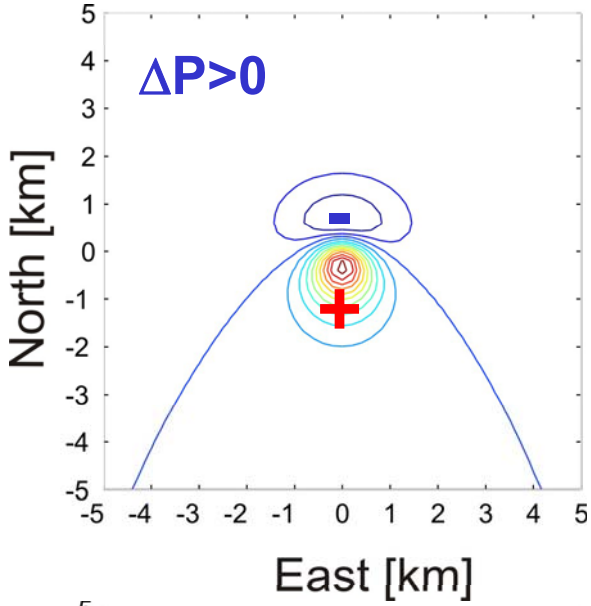

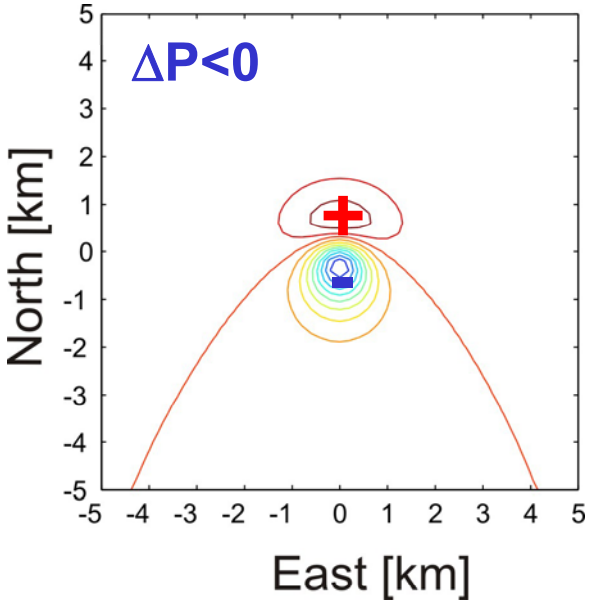

Thermomagnetic Effect

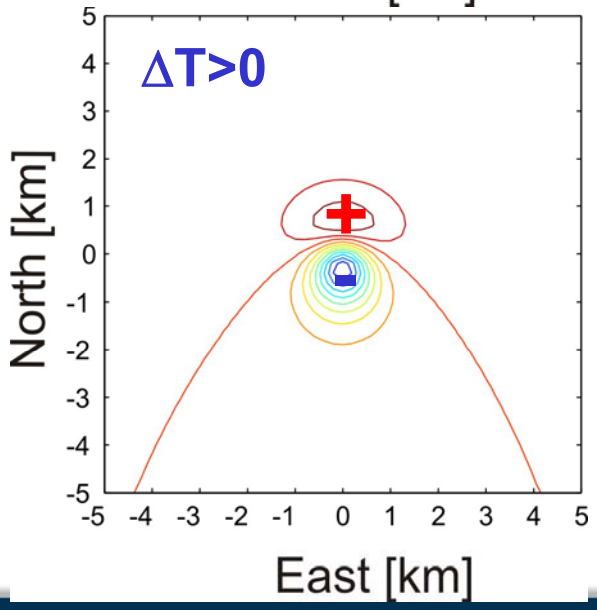

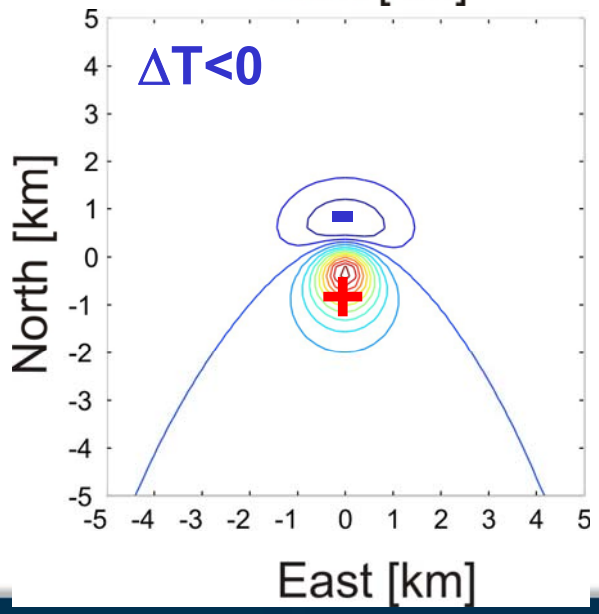

Piezomagnetic effetc in volcanic region

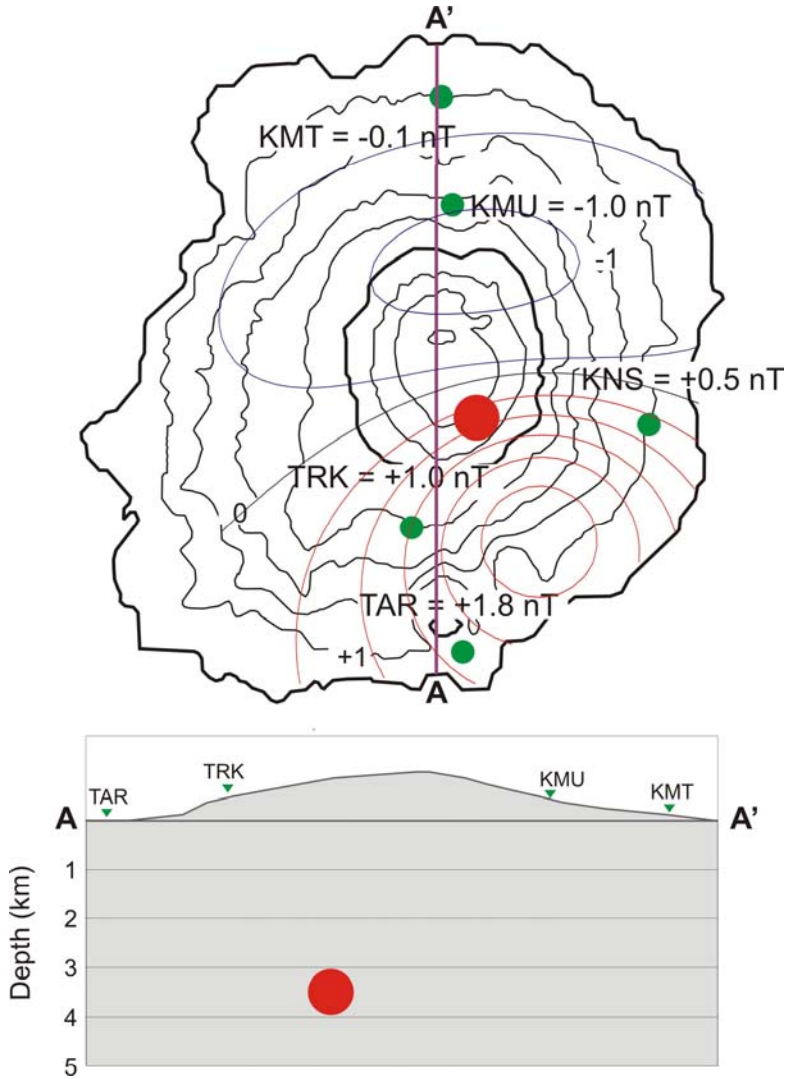

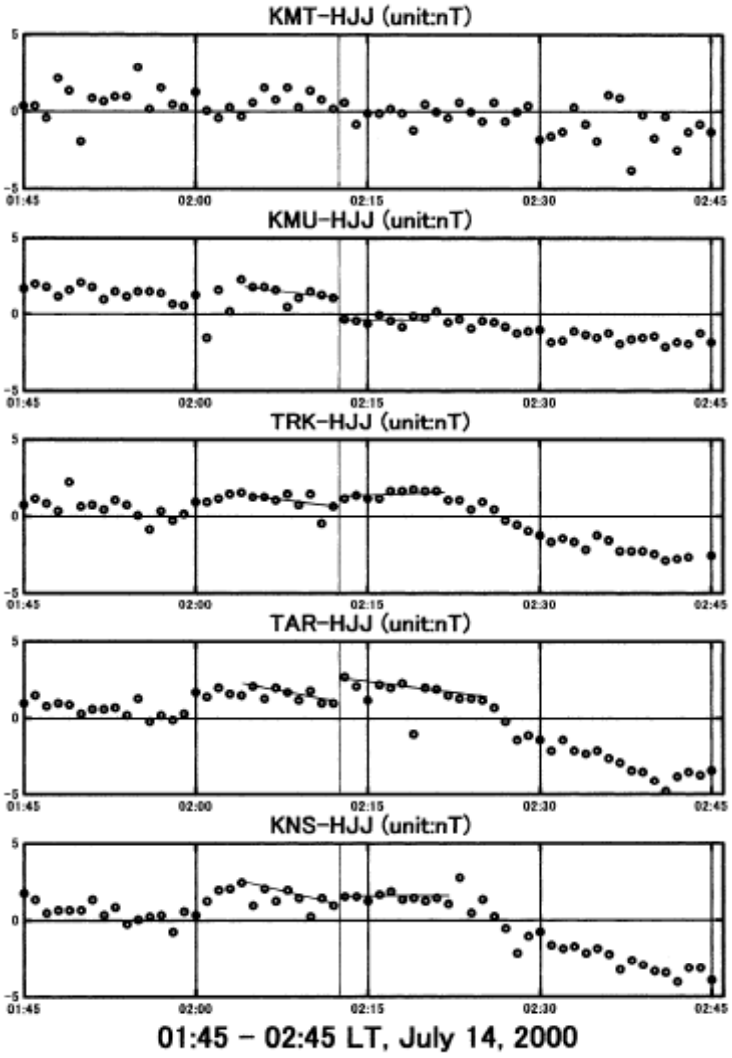

Sasai et al., 2002

Sezione di Catania

Istituto Nazionale di Geofisica e Vulcanologia

Polarity of volcanomagnetic changes

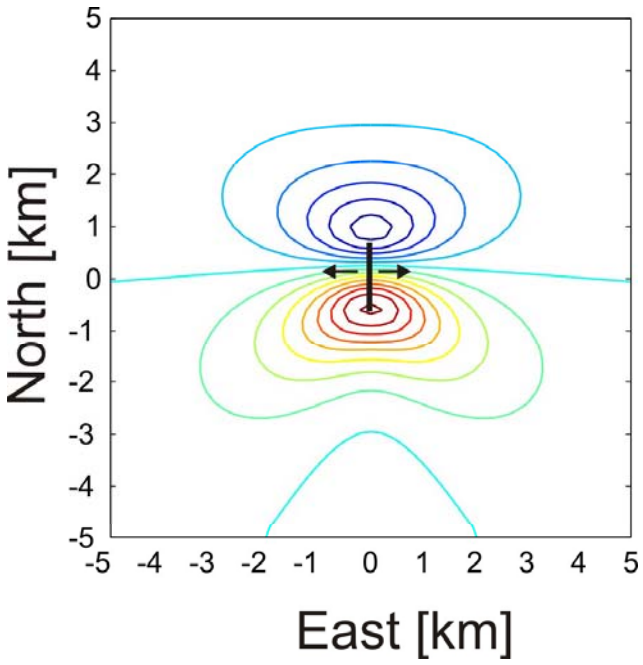

The stress- induced magnetization is proportional to the deviatoric stress $\boldsymbol{\sigma}'$ and the initial magnetization $\mathbf{J}$

$$\Delta \mathbf{J} = \frac{3}{2}\beta \boldsymbol{\sigma}' \mathbf{J}$$

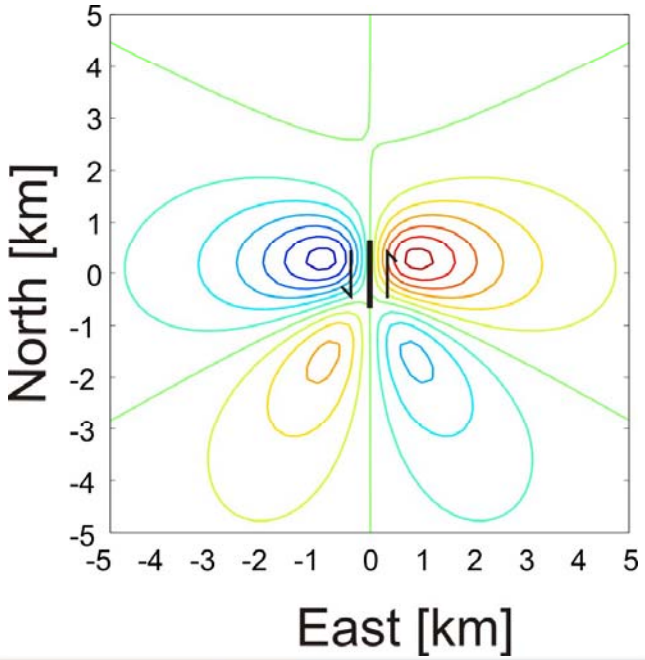

PiezoMagnetic Analytical Model
Mogi Source: Sasai, 1991
Dislocation Source: Utsugi et al. 2000

Sezione di Catania

Istituto Nazionale di Geofisica e Vulcanologia

Magnetic changes in seismic region

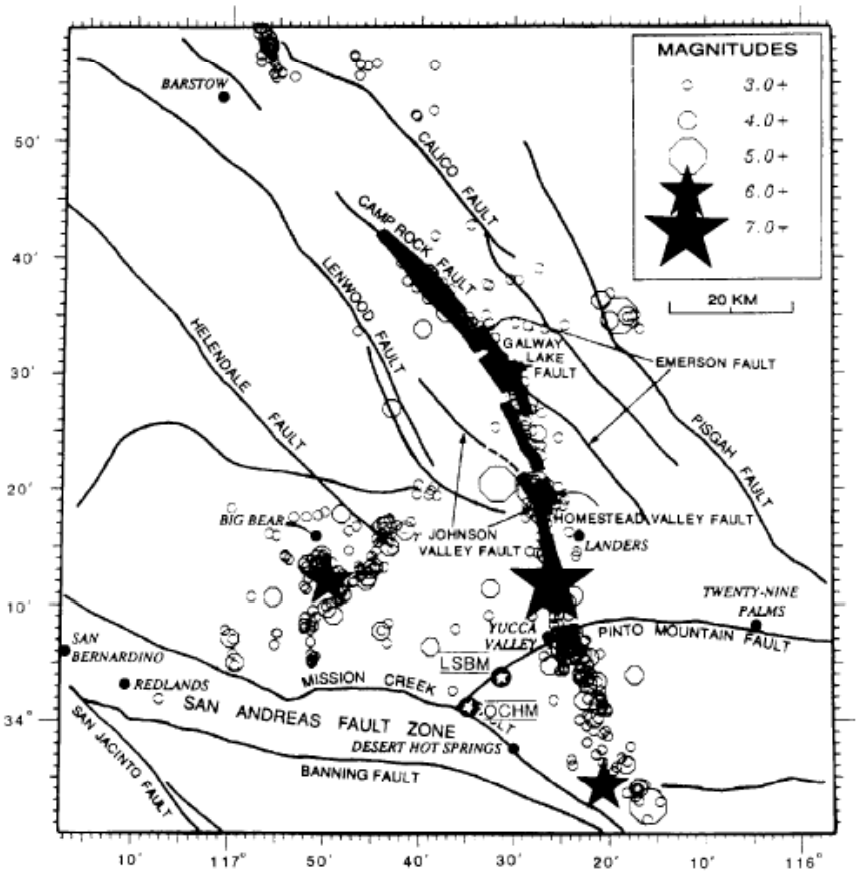

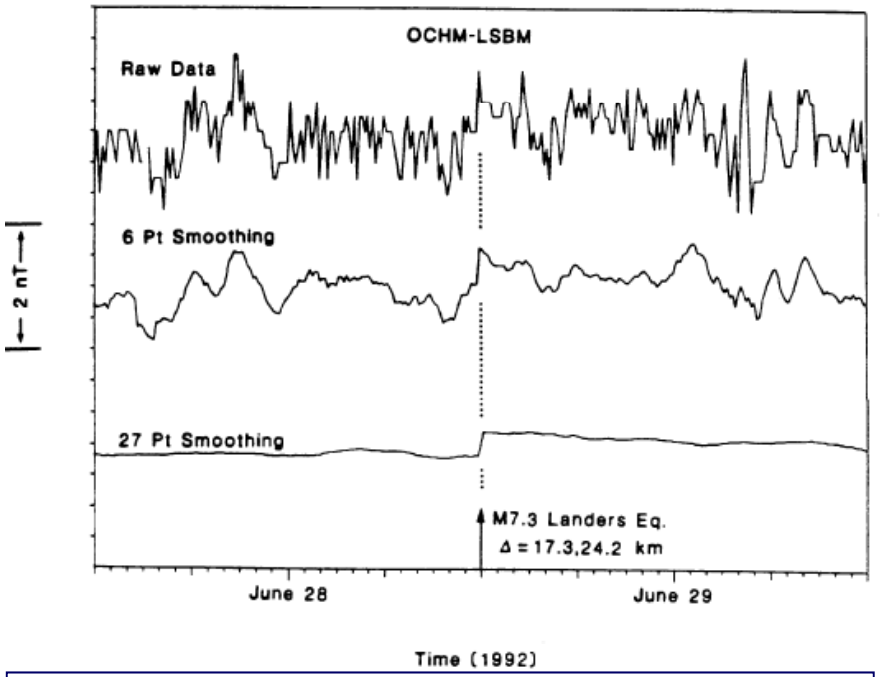

Differential magnetic field data encompassing the M 7.3 Landers earthquake on 28 June 1992

Muller and Johnston, 1998

Piezomagnetic effetc in seismic region

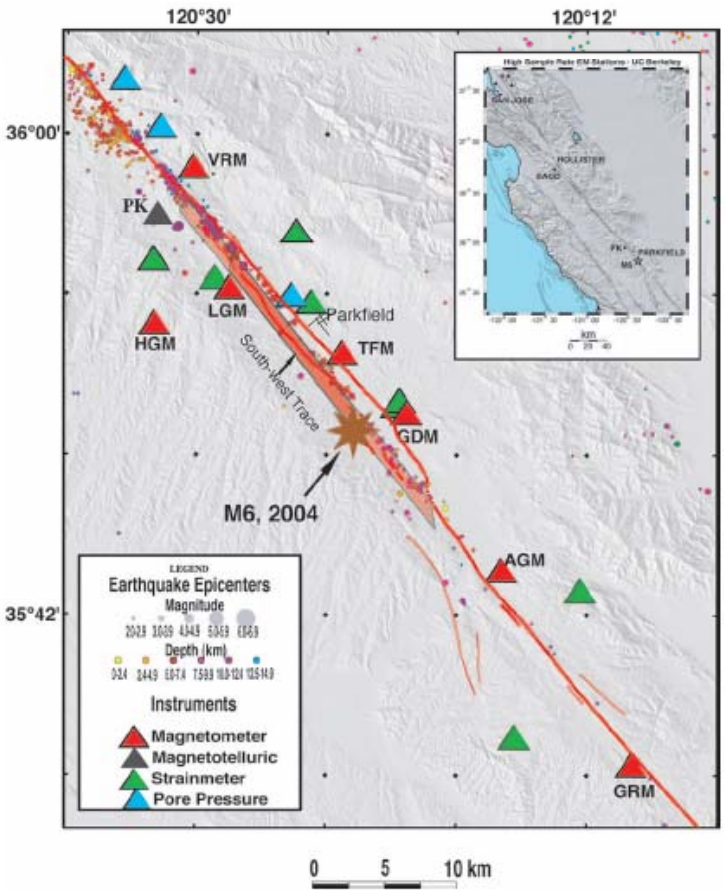

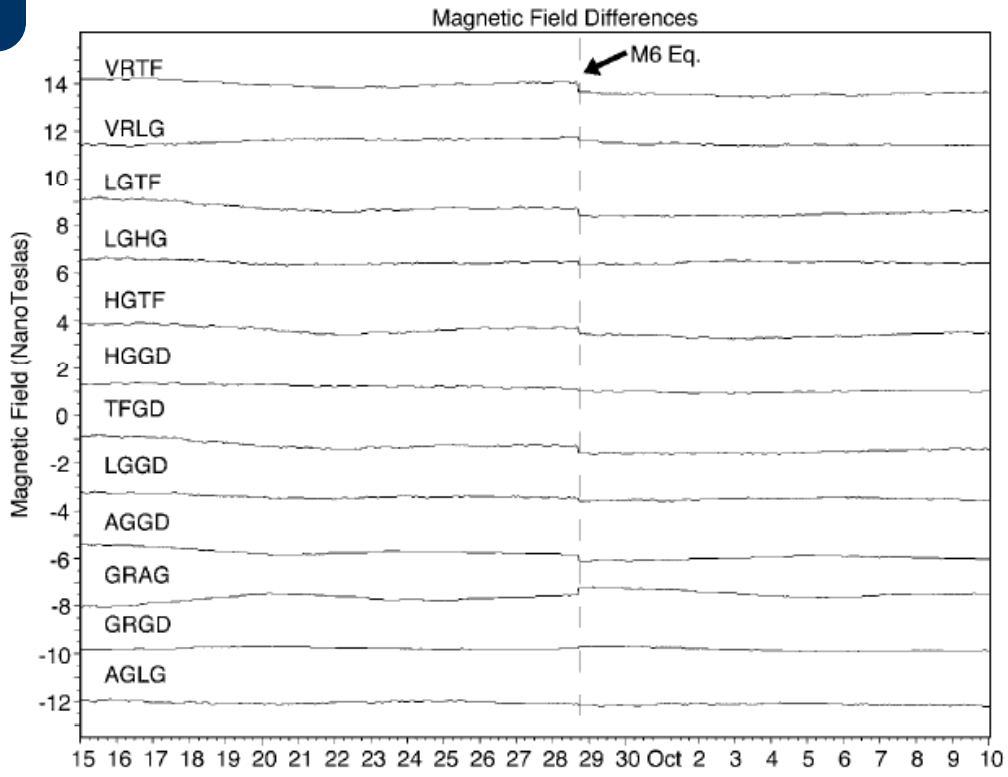

Differential magnetic field data encompassing the M 6 Parkfield earthquake on 28 September 2004

Johnston et al, 2006

Sezione di Catania

Istituto Nazionale di Geofisica e Vulcanologia

Deformation and Piezomagnetic model

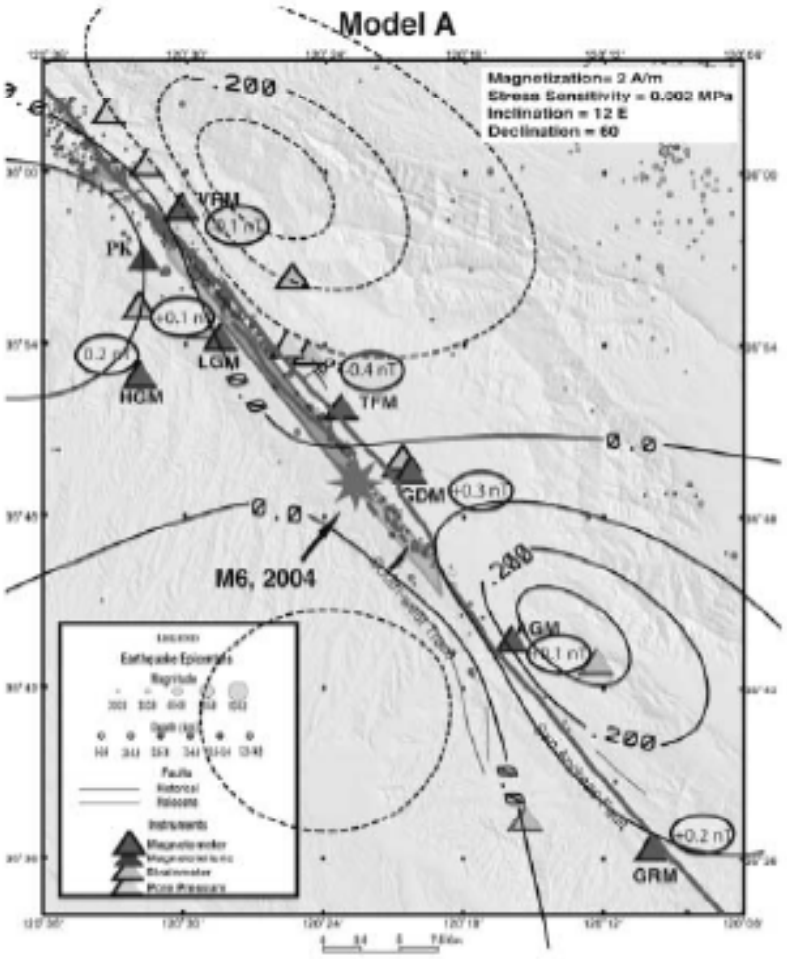

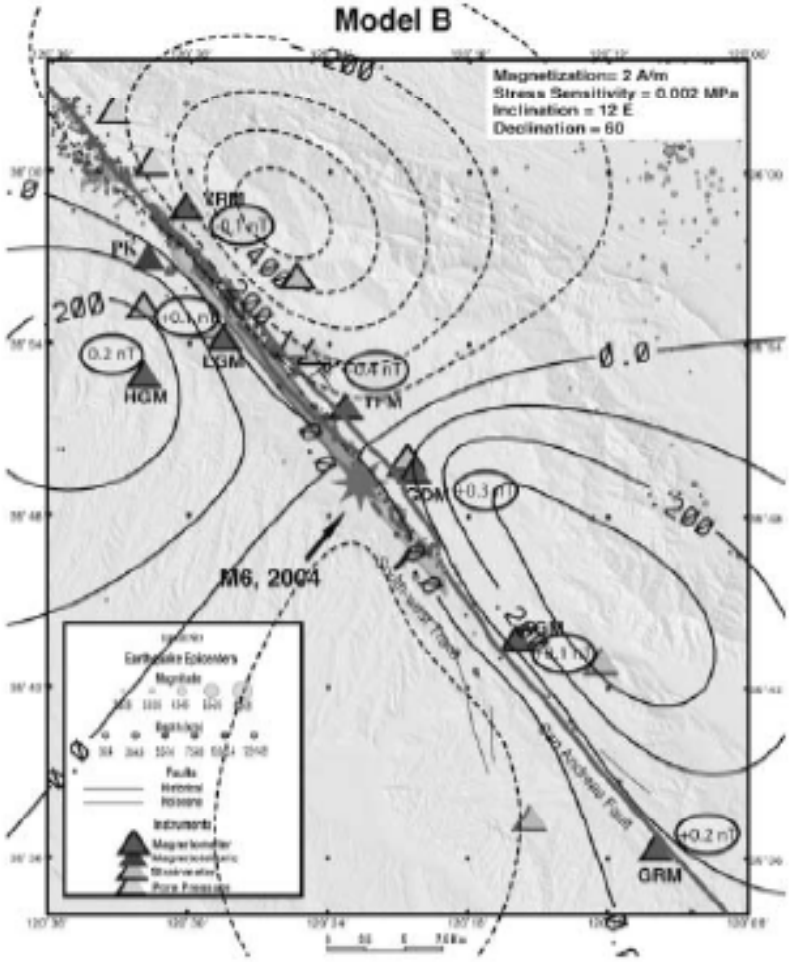

Sezione di Catania

Istituto Nazionale di Geofisica e Vulcanologia

Contributions to gravity anomaly

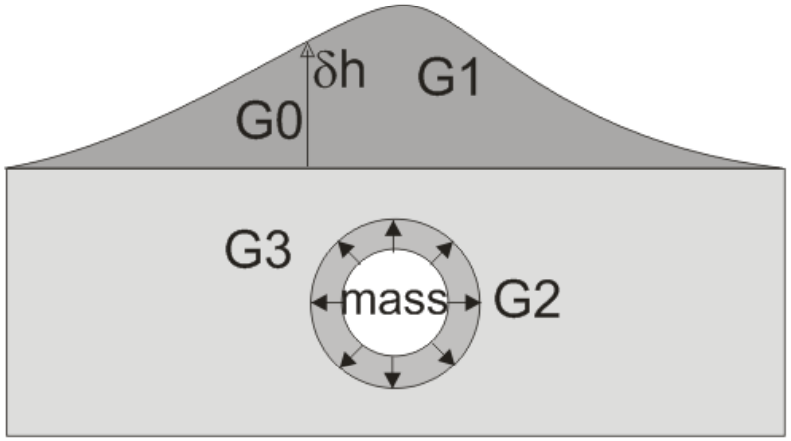

Gravity anomalies cannot be interpreted only in terms of additional mass input at some depth without taking into account the deformation of the surrounding rock required to host the magma volume.

$$\nabla^2 \phi_g = -4\pi G \Delta\rho(x,y,z)$$

$$\Delta g(x,y,z) = -\left(\frac{\partial \phi_g}{\partial z}\right) + \gamma_{FA} u_z$$

Analytical solutions have been provided by Okubo (1991, 1992, 1994) for dislocation and pressure source.

$$\Delta\rho(x,y,z) = \rho_m - \rho_0 \nabla \cdot \mathrm{u} - \mathrm{u} \cdot \nabla \rho_0$$

mass input: δg2

Volume change arising from compressibility of the surrounding medium: δg_3

Displacement of density boundaries in heterogeneous media: δg_1

Gravity and Magnetic network at Etna

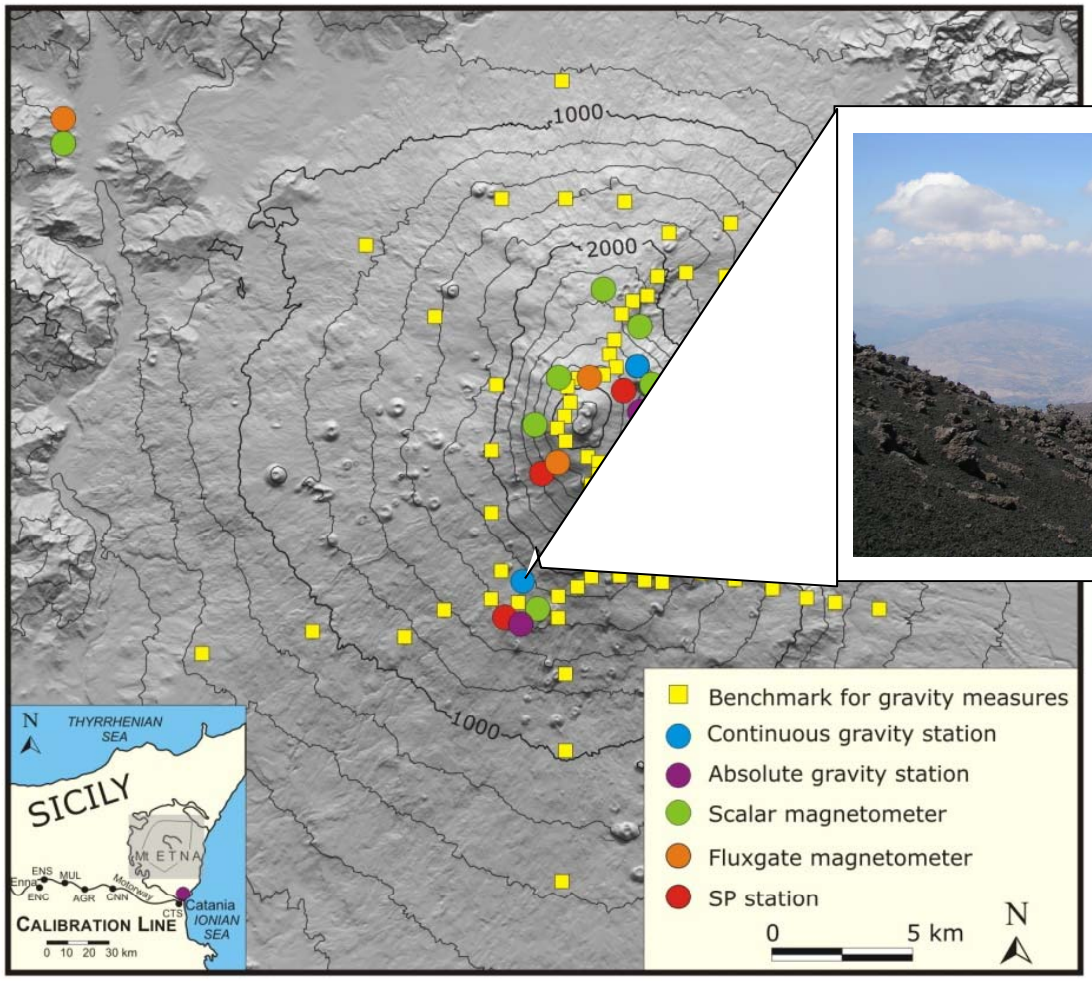

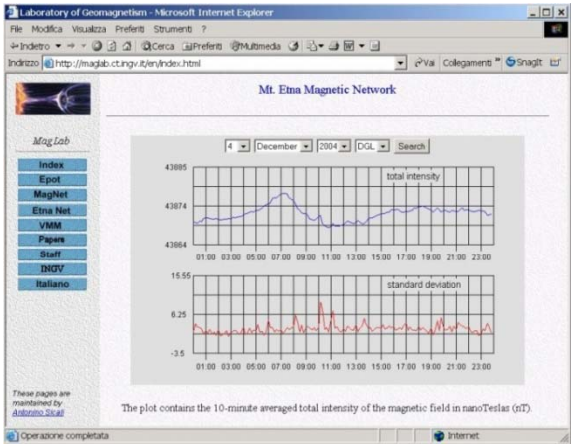

WEB Site: http://www.ct.ingv.it

Sezione di Catania

Istituto Nazionale di Geofisica e Vulcanologia

Review of 1981 eruption at Etna

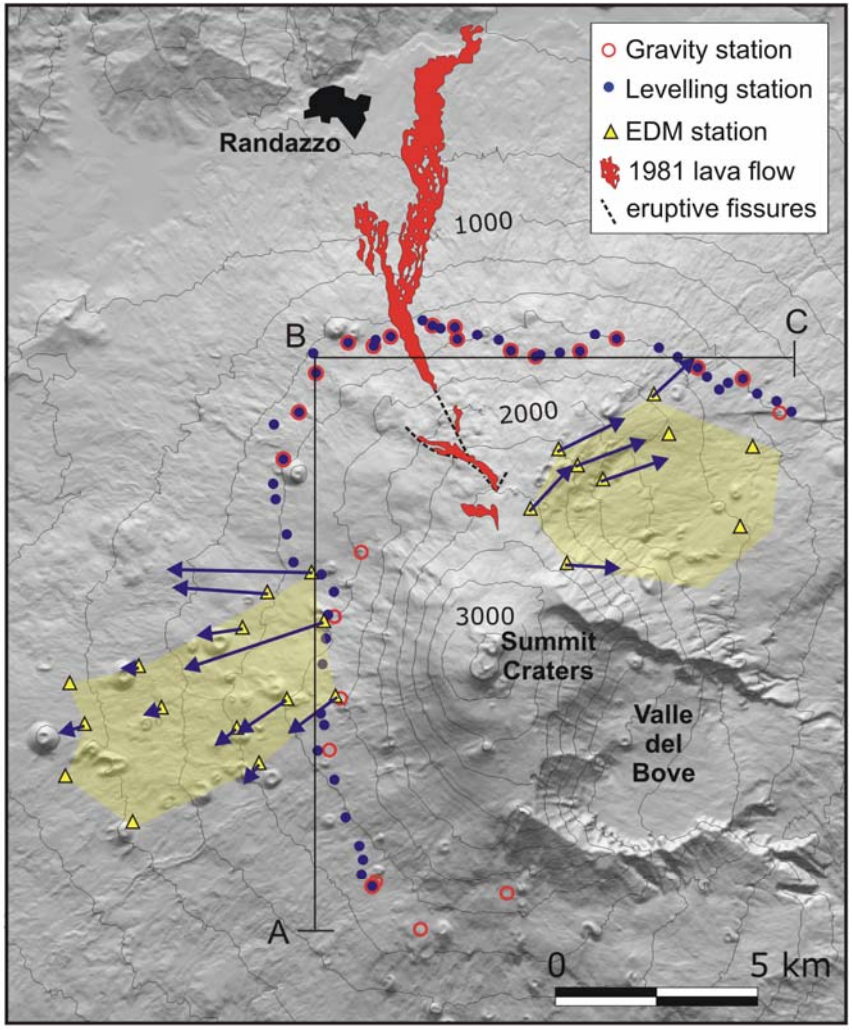

Sanderson et al. [1983] performed a joint analysis of the microgravity and leveling data covering the August/September 1980 - July/August 1981 period

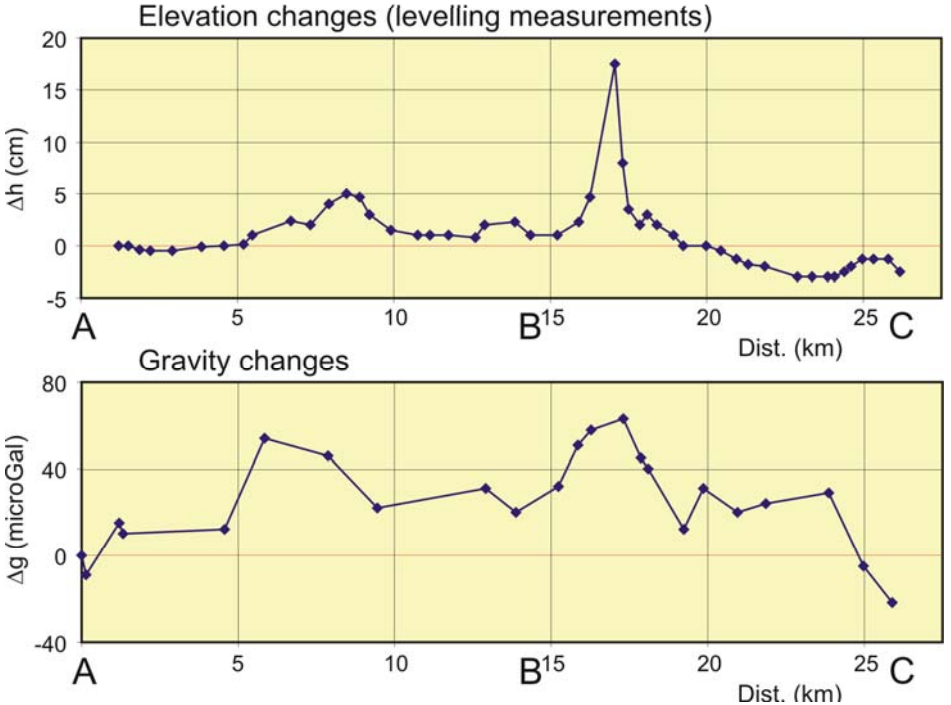

Sezione di Catania

Istituto Nazionale di Geofisica e Vulcanologia

Gravity and deformation model

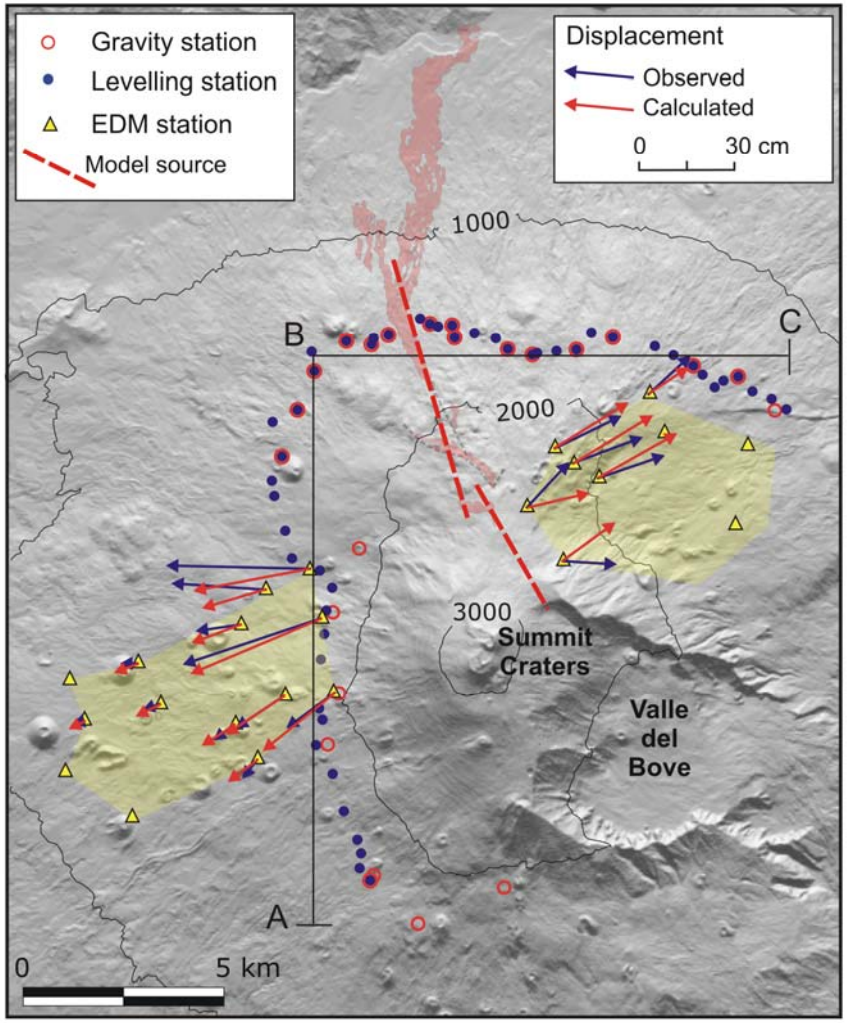

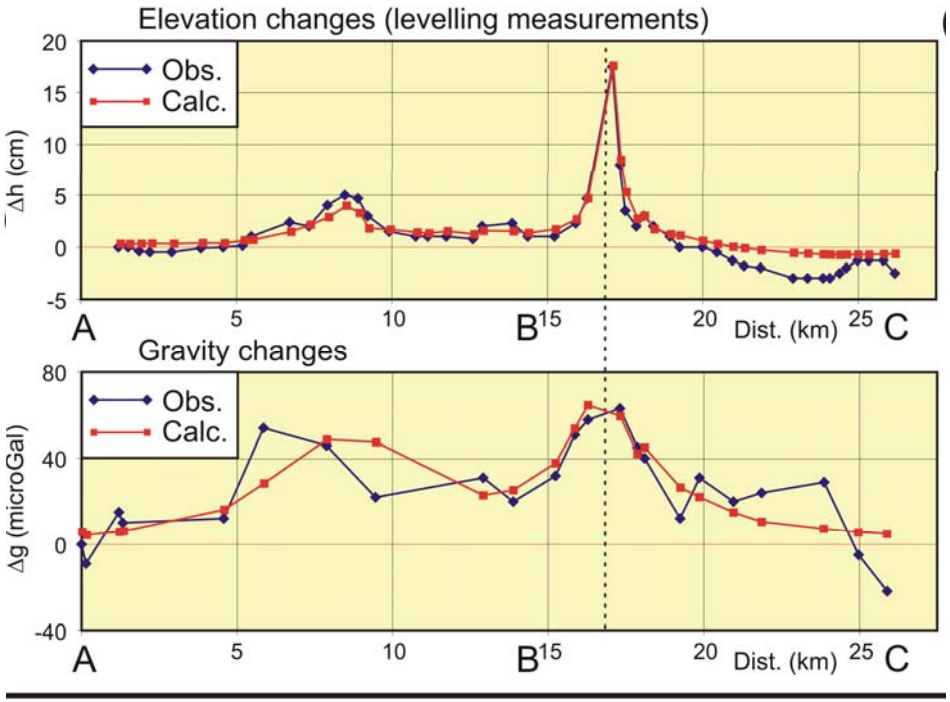

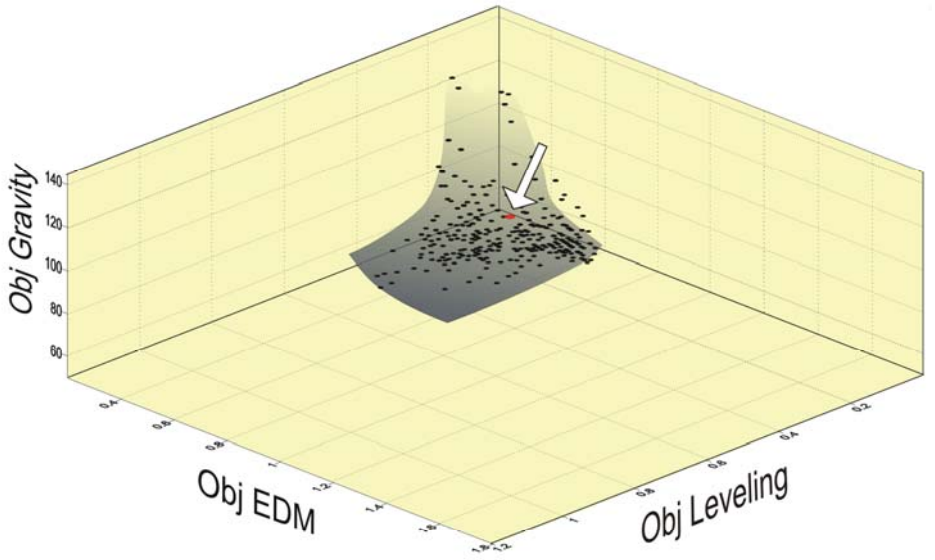

Carbone et al., 2008

Sezione di Catania

Istituto Nazionale di Geofisica e Vulcanologia

Sezione di Catania

Etna 2002-2003 Eruption

Istituto Nazionale di Geofisica e Vulcanologia

Eruptive Activity

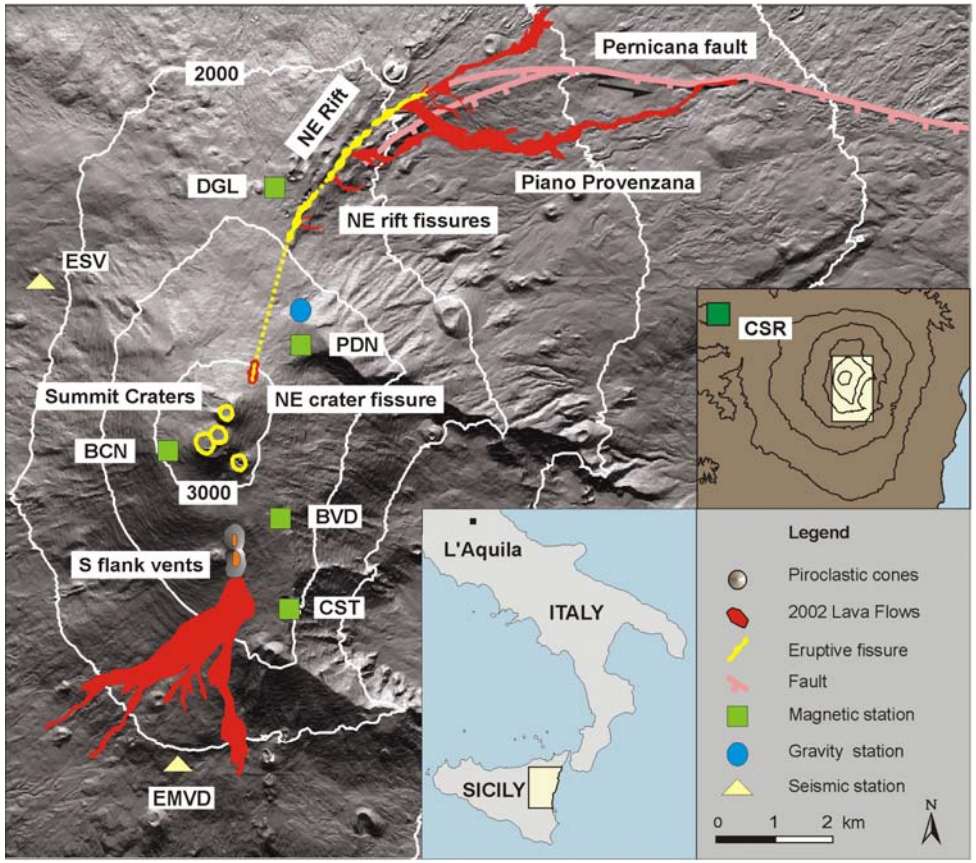

On October 26, 2002 at 22:25 a strong seismic swarm, took place in the central upper part of Mt. Etna and several hours later powerful lava fountains and ash columns occurred on the south flank, along a N-S fracture field.

About 5 hours later, on October 27, another eruptive fracture system opened on the northeastern flank, nearly to the NE Rift.

Sezione di Catania

Istituto Nazionale di Geofisica e Vulcanologia

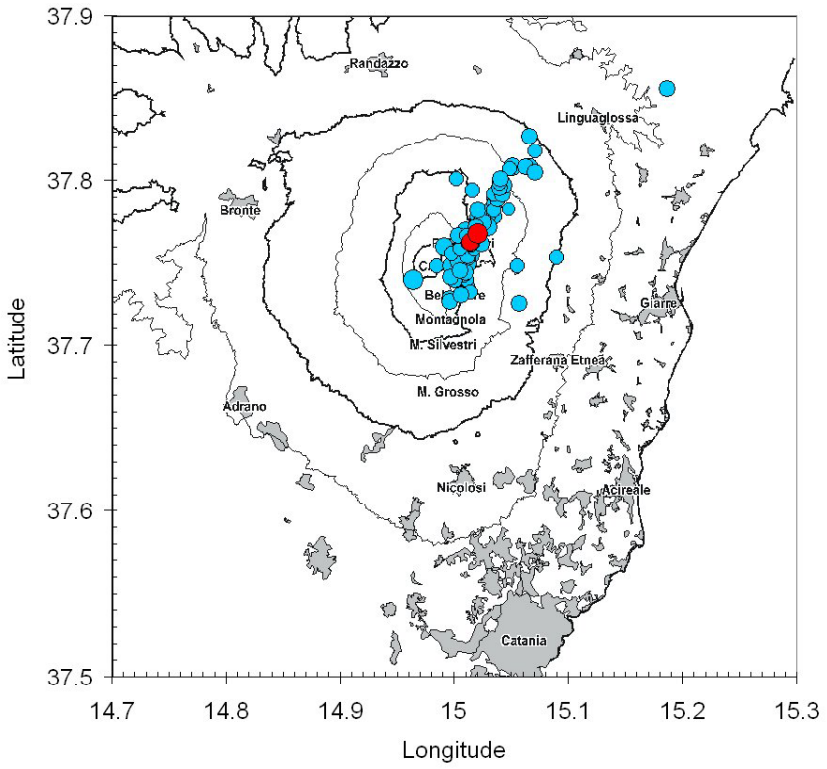

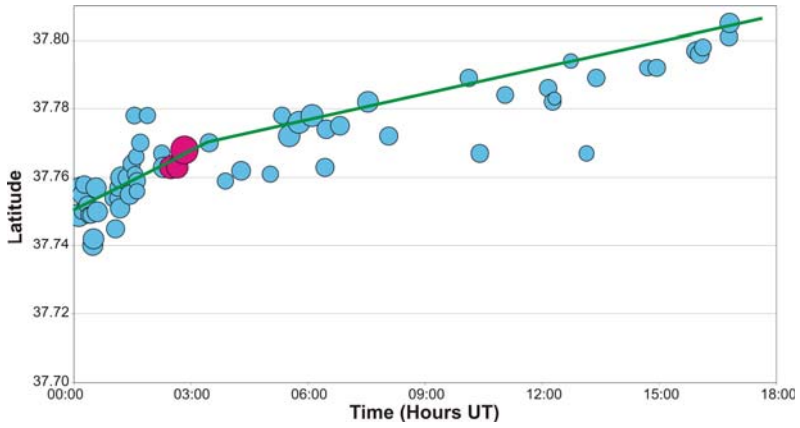

The epicentral migration toward the northeast suggested that the seismicity in the North-East Rift is a consequence of dike propagation.

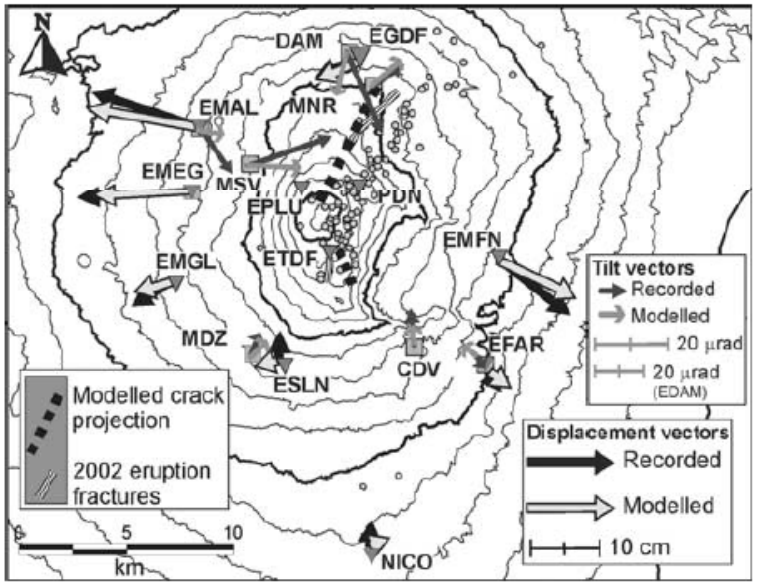

The deformation pattern was consistent with a response of the edifice to a vertical dike rising in the southern flank and a radial intrusion in the NE sector.
Aloisi et al., 2003

Daily Magnetic Field Variations

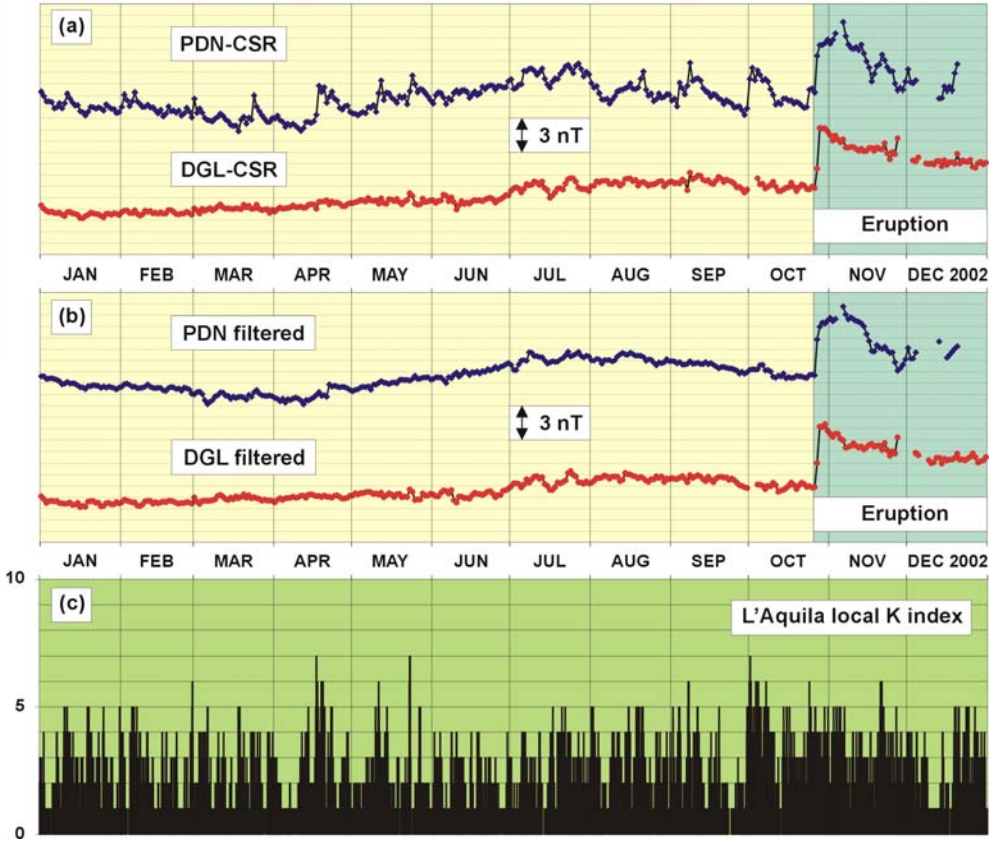

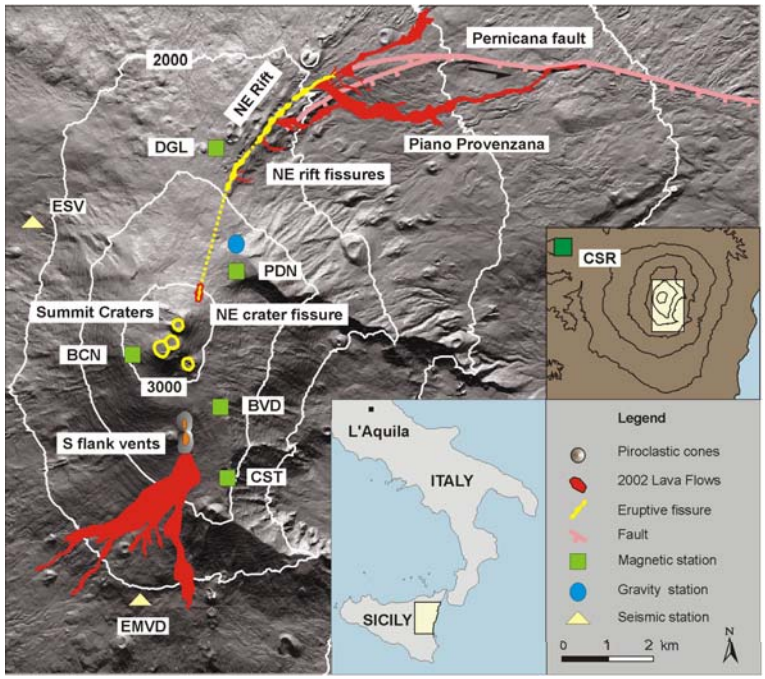

After having removed external fluctuations using adaptive filtering, no noticeable precursory long-term signal is detected before the eruption, whereas remarkable short-time changes anticipated and accompained the openings of the eruptive fissures.

Sezione di Catania

Istituto Nazionale di Geofisica e Vulcanologia

Timing the 2002 Etna Eruption Onset

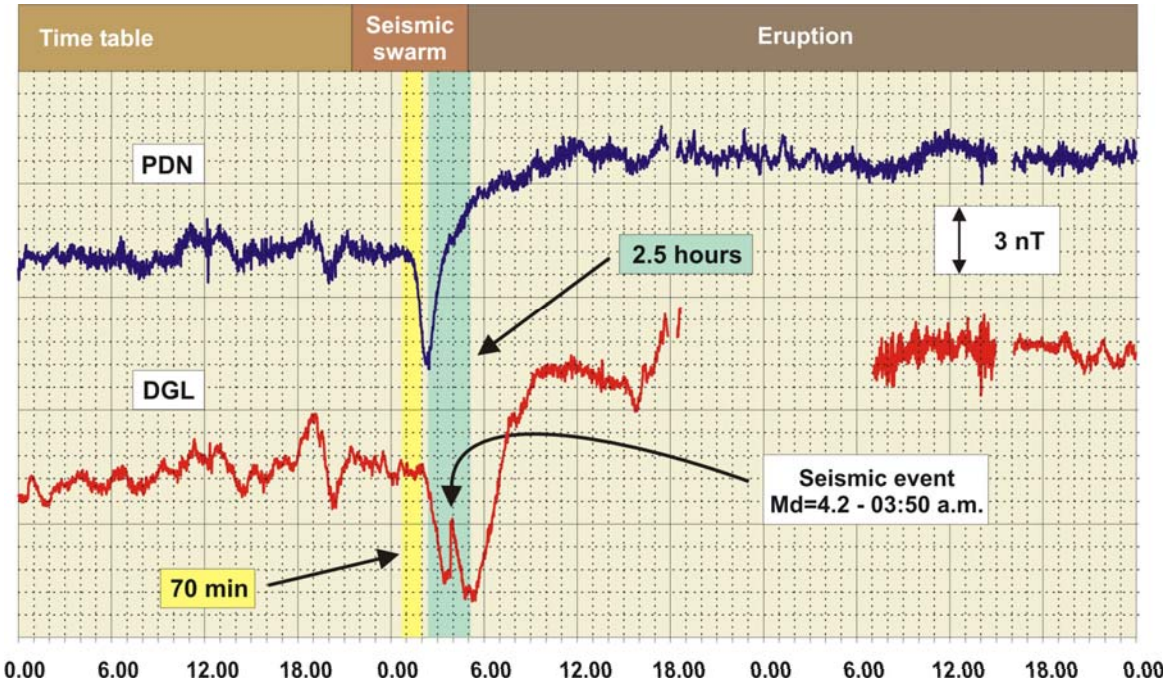

Two stages are recognized in the magnetic field changes:

- a faster negative variations at PDN and DGL stations
- a slower positive variations at both stations.

A delay of about 70 minutes is observed between the minimum of the two signals.

The local magnetic fields at PDN and DGL stations allowed also timing the onset of the eruption. The most significant change in the magnetic field is associated with the opening and propagation of the vents along the NE Rift.

Del Negro et al., 2004

Magnetic and Seismic Events

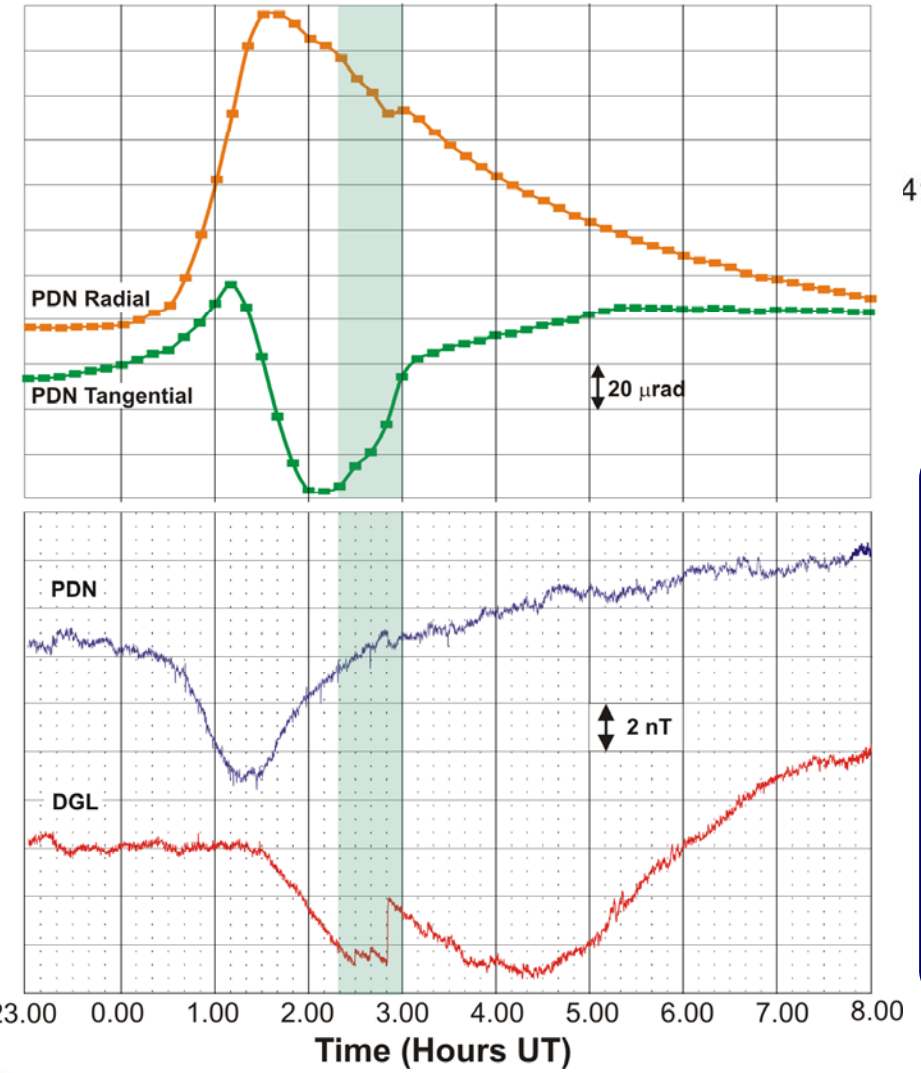

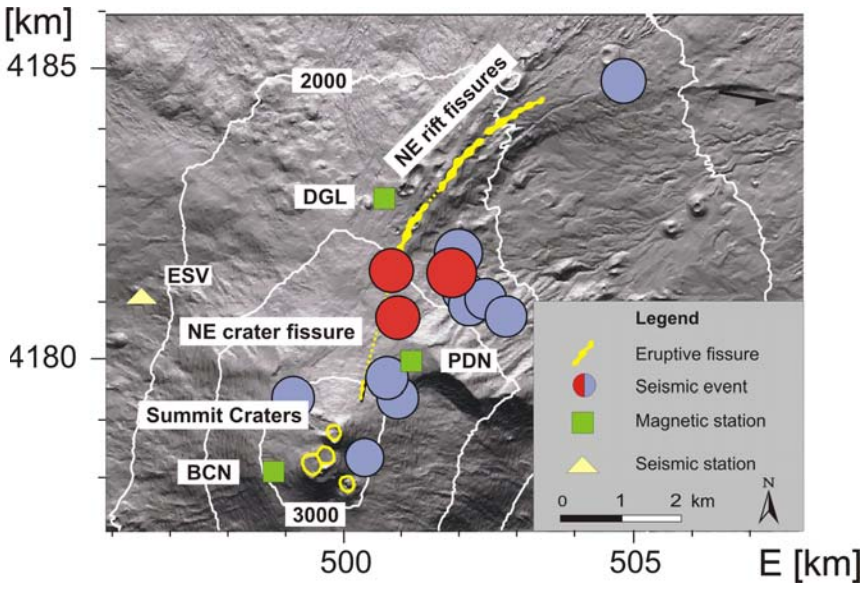

Geophysical data interpretations point out that the changing stress field induced by the dike intrusion proportionally controls the seismicity rate during earthquake swarms. The seismicity related to the magma intrusion along the North-East Rift indicated an abrupt stress change that could have triggered the earthquakes and driven the magnetic changes.

Currenti et al., JGR 2008

Sezione di Catania

Istituto Nazionale di Geofisica e Vulcanologia

2002 Etna Eruption: Magnetic Timetable

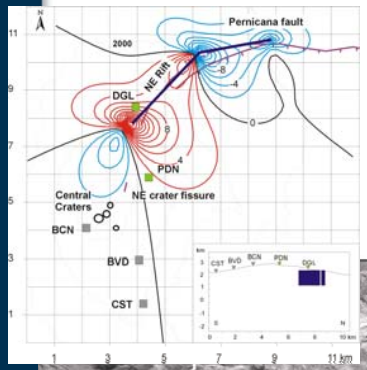

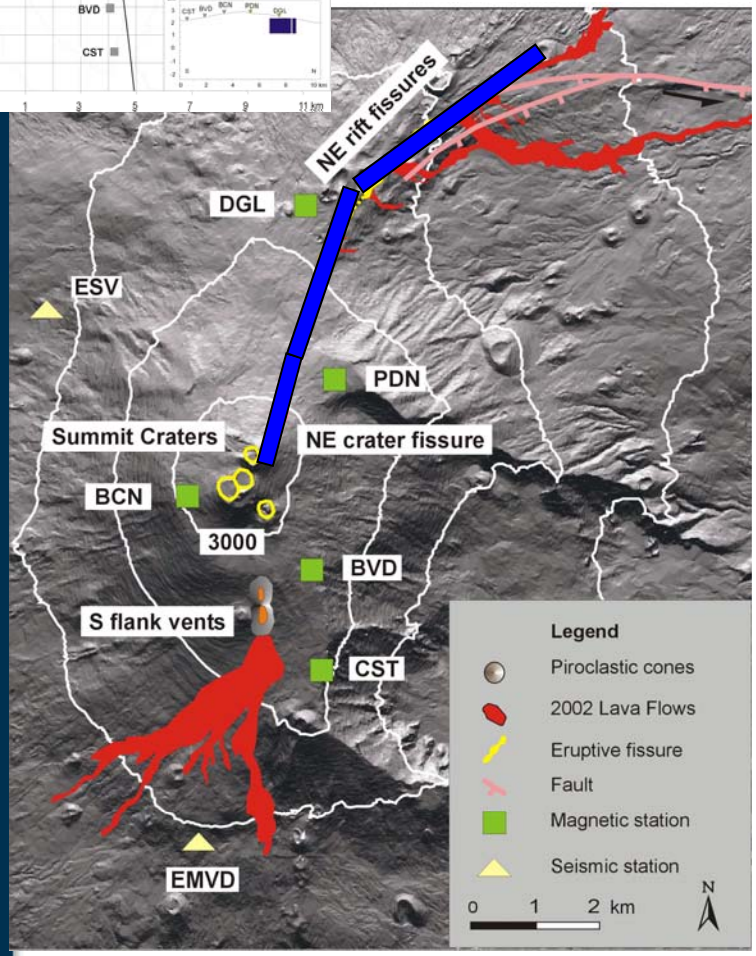

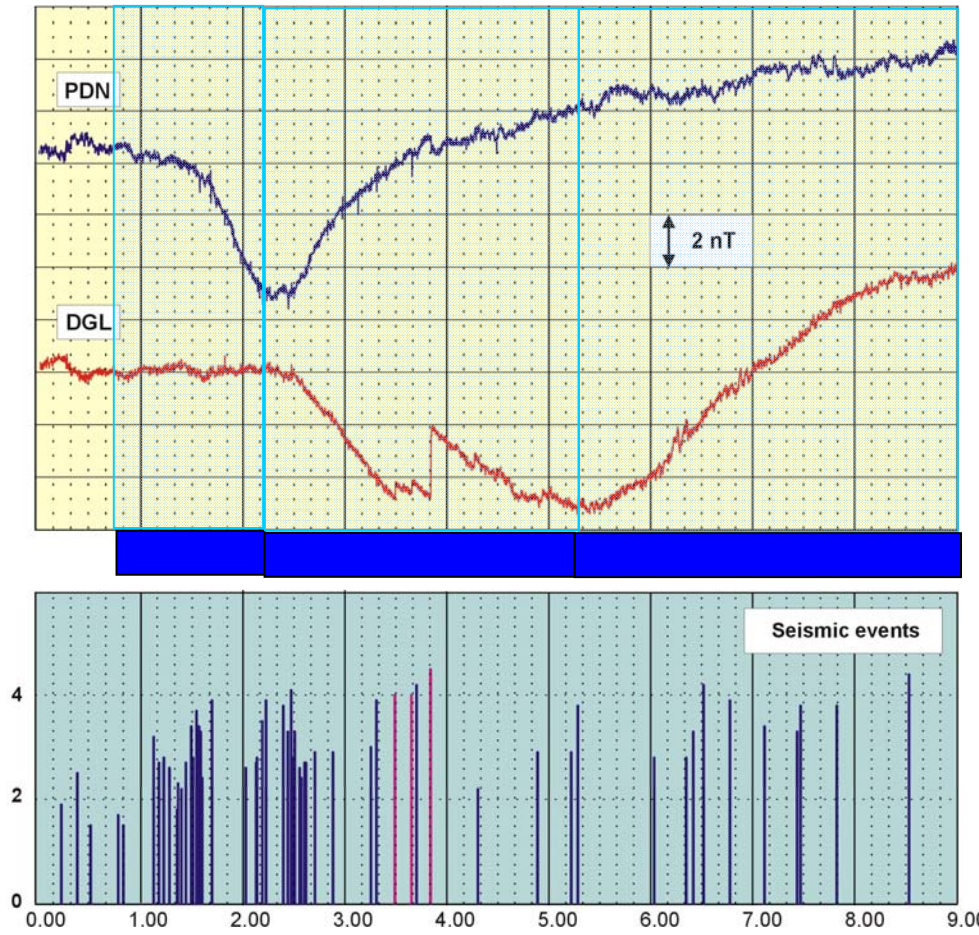

Del Negro et al., EPSL 2004

Sezione di Catania

Istituto Nazionale di Geofisica e Vulcanologia

3D FEM of Mt Etna

A fully 3D Finite Element Model of Mt Etna is carried out using **Pylith** code (CIG, USA), **Lagrit** and **COMSOL Multiphysics** to include:

- ✓ **The Real Topography**
- ✓ **The Medium heterogeneities**

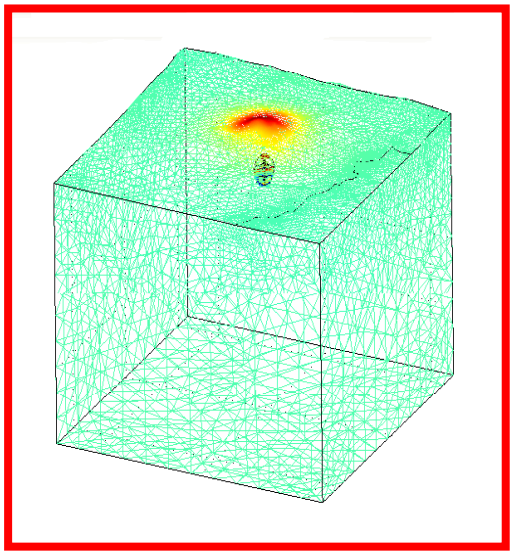

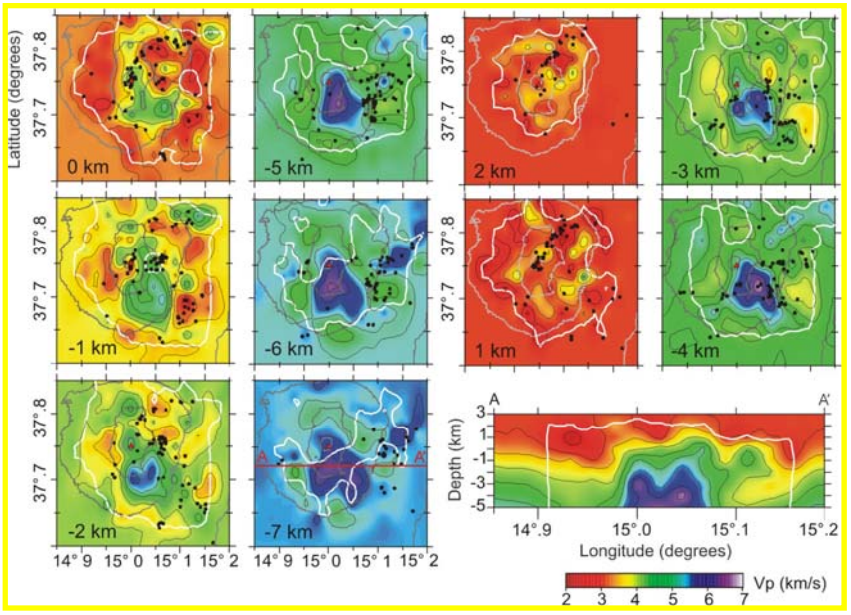

The subsurface elastic heterogeneities of the medium were estimated by using recent seismic tomographic investigations (Patanè et al 2006).

Sezione di Catania

Istituto Nazionale di Geofisica e Vulcanologia

Numerical Piezomagnetic Model

Deformation modelling → **Numerical solution of deformation field**

Poisson equation → **Piezomagnetic and Gravity fields**

Gravity

$$\nabla^2 \phi_g = -4\pi G \Delta\rho(x,y,z)$$

$$\Delta g(x,y,z) = -\left(\frac{\partial \phi_g}{\partial z}\right) + \gamma_{FA} u_z$$

Piezomagnetic

$$\nabla^2 \phi_m = 4\pi \nabla \cdot \Delta \mathbf{J}$$

$$\Delta J_{ij} = \beta\mu \left\{ -\delta_{ij} \nabla \cdot \mathbf{u} + \frac{3}{2}\left(\frac{\partial u_j}{\partial x_i} + \frac{\partial u_i}{\partial x_j} \right) \right\} J_j$$

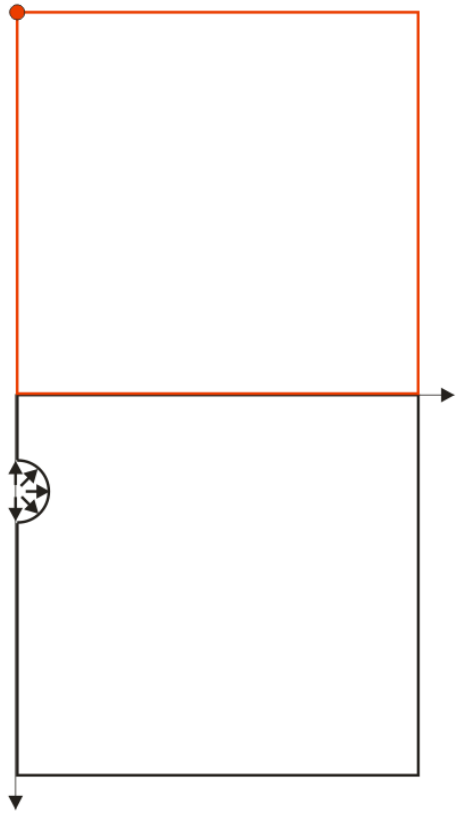

In order to solve the Poissons equation the potential or potential derivative are to be assigned at the boundaries of the domain (Dirichlet or Neumann boundary conditions), which is extended along the z direction of 50 km to finally obtain a 100x100x100 km computational domain. Along the external boundaries the magnetic field is assumed to be tangential by assigning a Neumann condition on the magnetic potential. The problem is made unique by setting the potential to zero at an arbitrary point on the external boundary. The continuity of the magnetic potential on the ground surface is also warranted.

Effects of elastic medium heterogeneity on piezomagnetic field

Firstly, we evaluated the effect of elastic heterogeneity on the piezomagnetic field while the magnetic properties are assumed homogeneous.
Successively, models with heterogeneous distribution of initial magnetization, but homogeneous in elastic properties were also investigated.

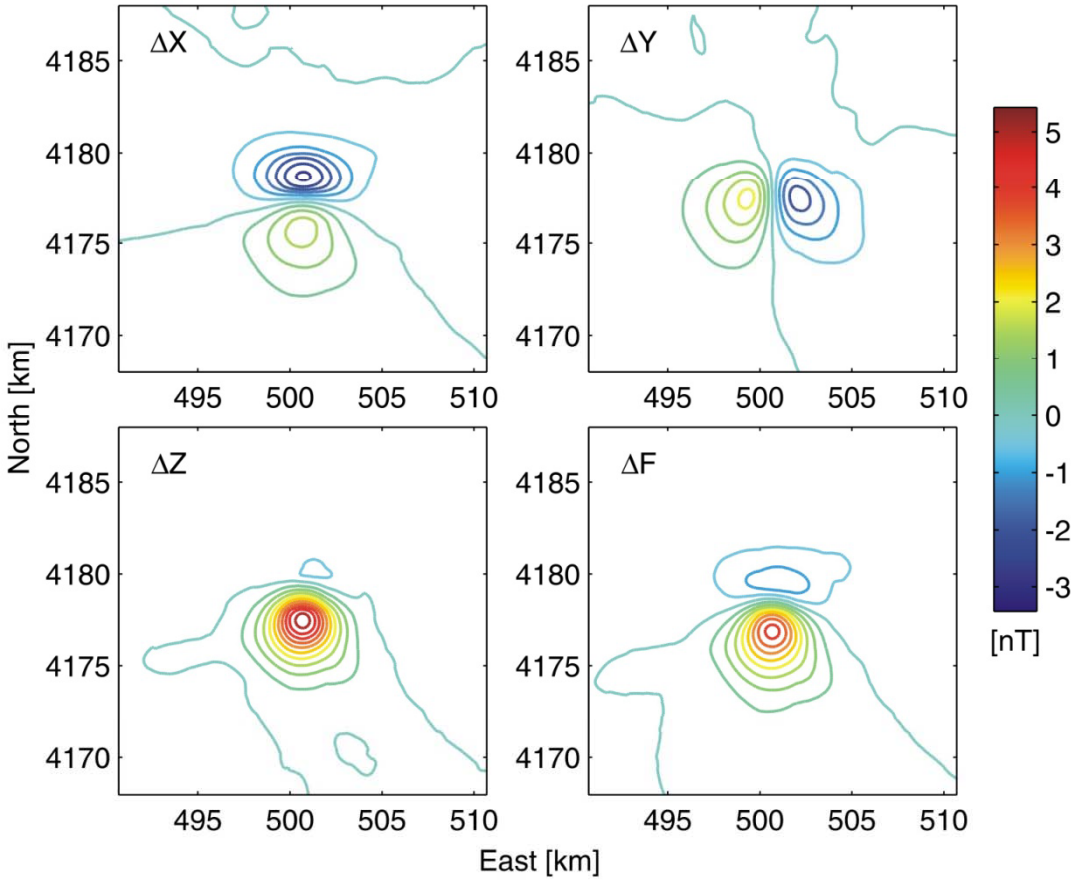

Three components and total intensity of piezomagnetic anomaly produced by a pressurized source for an half-space, which is homogeneous in magnetic properties and heterogeneous in elastic parameters. Contour lines are at 0.5 nT intervals.

Effects of magnetic heterogeneity on piezomagnetic field

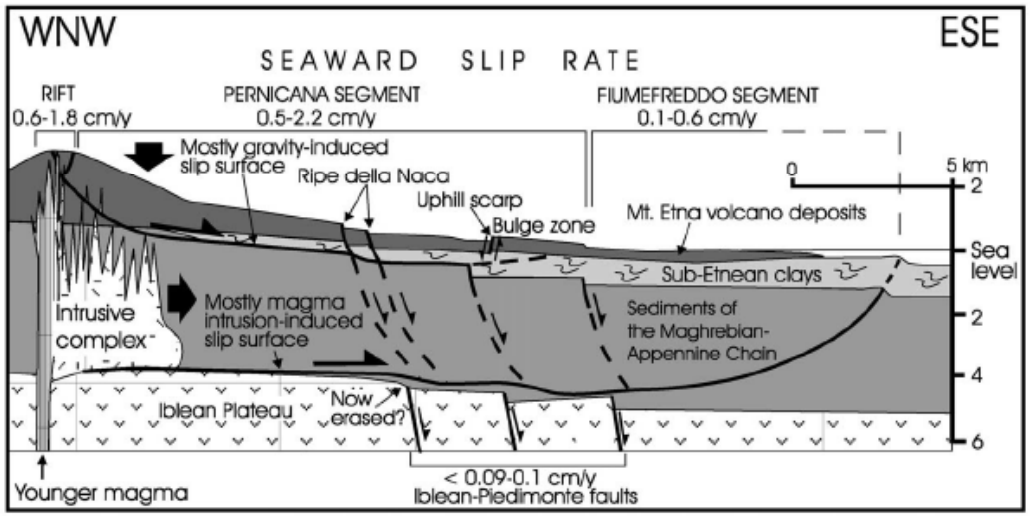

Fig. 17. Interpretative WNW–ESE sketch section of the structures affecting the NE flank of Mt. Etna. We propose the presence of two main surfaces which enable the seaward shift of the Mt. Etna eastern flank. The upper surface has a listric shape with an U-shaped cross-section and guides mainly mass-induced sliding of the cone flank. The deeper sub-horizontal surface allows eastward shift of the volcano flank in order to provide space for the intrusive complex (Borgia et al., 1992; Rust and Neri, 1996). Our new detailed data on slip rates of all the structures of the NE volcano flank suggest the contemporary presence of both surfaces which can move alternatively or can move at the same time by a combination of effects. Our interpretation also considers the PF as the surface expression of the lateral ramp of the upper slip surface and the Pernicana–Fiumefreddo system as the lateral ramp of the deeper sliding surface, in accordance with slip rates. Tectonic faults of the Timpe–Ibleo–Maltese system and of Piedimonte have been projected on the section from the nearest outcrops. Other minor structures can represent the surface effect of slippage of the volcano flank above fault steps of the basement. Section trace in Fig. 1.

Generally in a volcano such as Etna, built up by a stack of basic lavas, magnetizations are frequently high. Considering the tomographic modelling of Etna plumbing system obtained by Chiarabba et al. (2000) and the geological based models by Tibaldi and Groppelli (2002), we evaluated two different layered half-space structure.

Effects of magnetic heterogeneity on piezomagnetic field

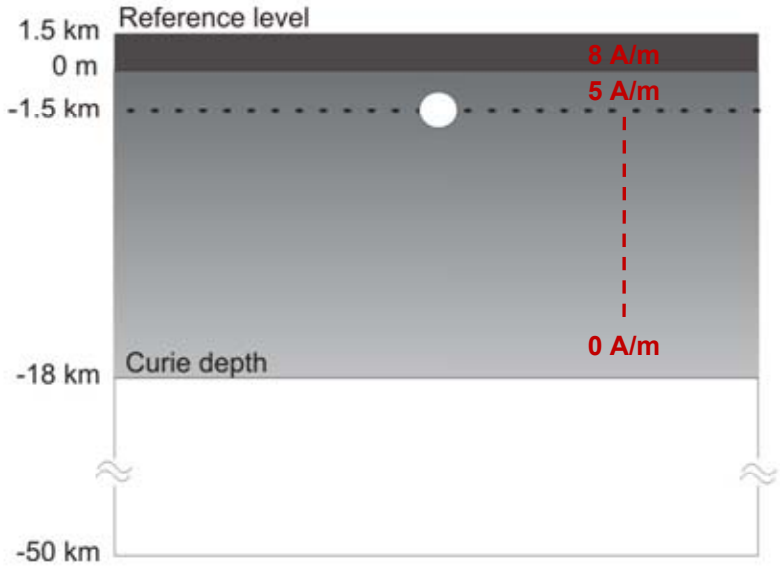

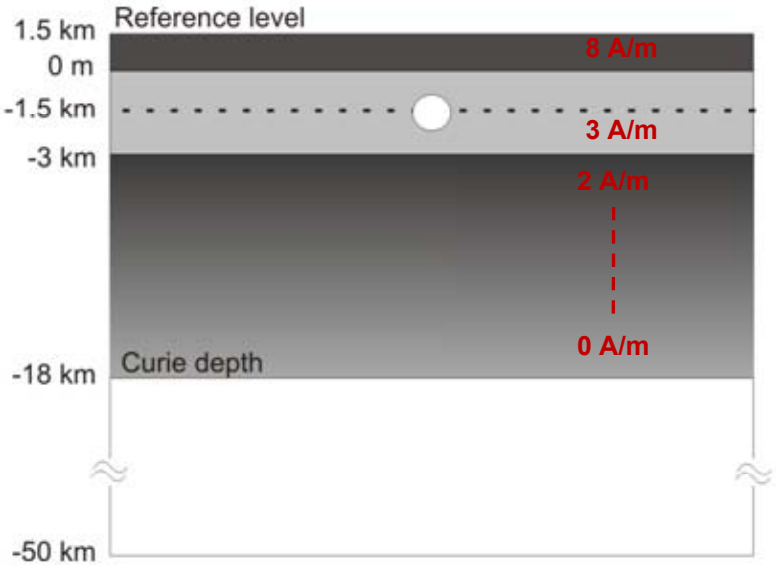

We assumed a high magnetization value for the volcano edifice lying on a substrate with lower magnetization. Particularly, we considered two half-spaces with different layers and magnetic properties, thereafter referred as J_A (on the left) and J_B (on the right).

$$J = \begin{cases} J_0\sqrt{1-\left[(0.03(z_0 - z)+10)/T_c\right]^2} & z_0 - z \geq \dfrac{T_c - 10}{0.03} \\ 0 & z_0 - z < \dfrac{T_c - 10}{0.03} \end{cases}$$

Effects of magnetization heterogeneity on piezomagnetic field

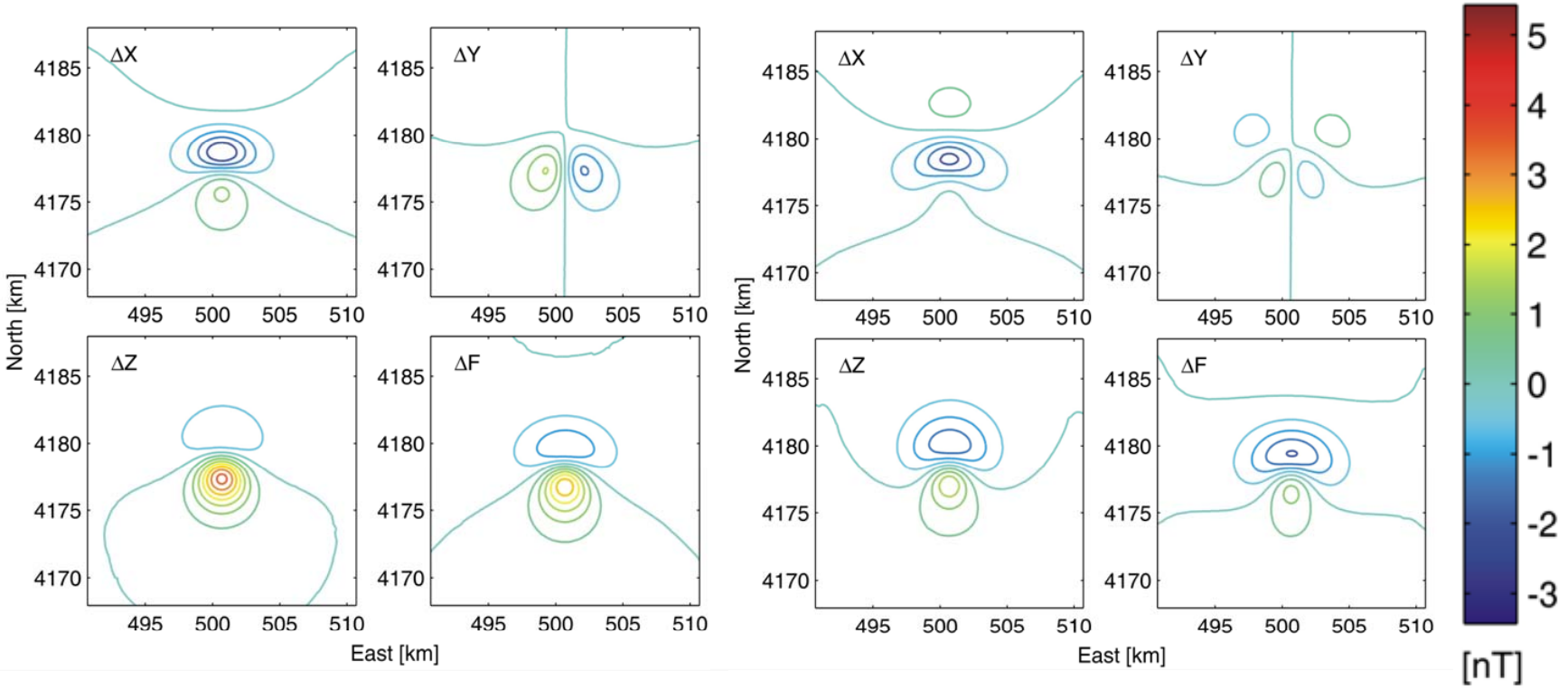

Three components and total intensity of piezomagnetic anomaly produced by a pressurized source for the half-space models J_A (on the left) and J_B (on the right)

Effects of magneto-elastic heterogeneity on piezomagnetic field

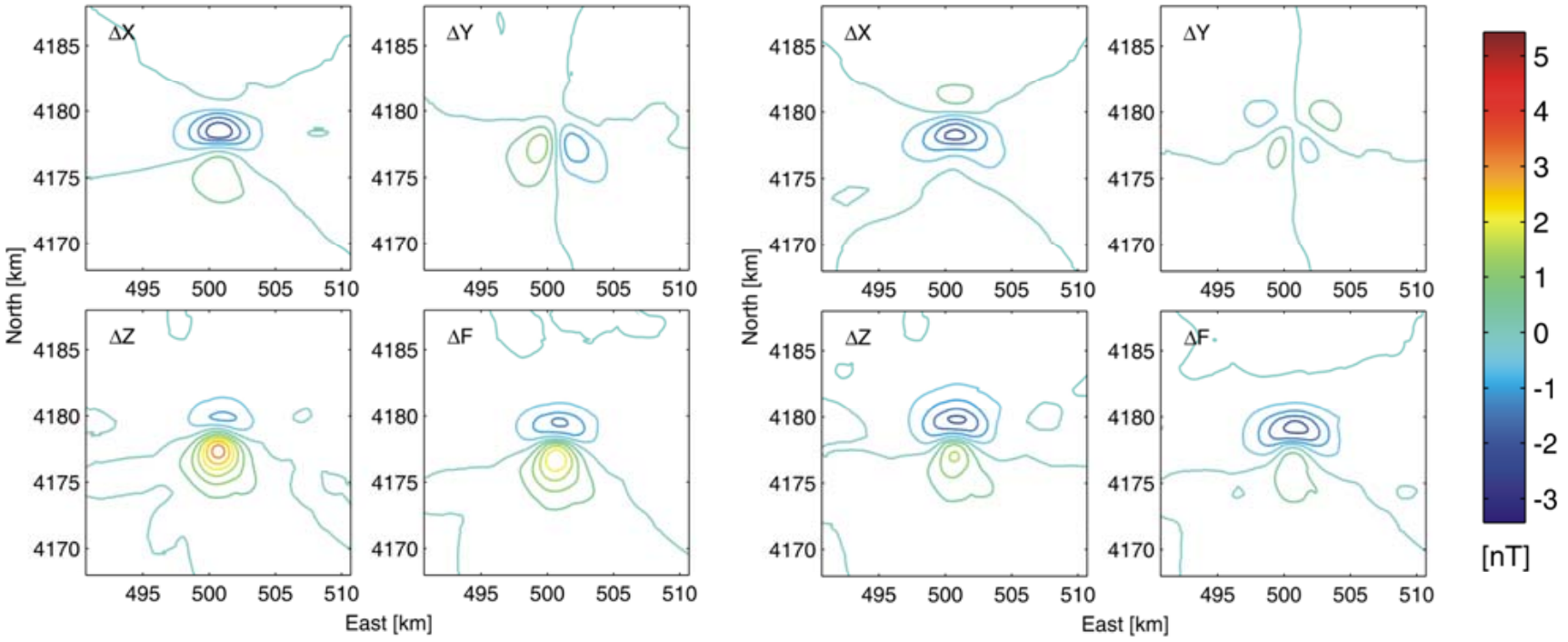

Three components and total intensity of piezomagnetic anomaly produced by a pressurized source for the half-space models J_A (on the left) and J_B (on the right). The elastic medium heterogeneity is also included.

Effects of topography on piezomagnetic field

The ground surface was generated using a digital elevation model of Mt Etna from the 90 m SRTM data and a bathymetry model from the GEBCO database. The computational domain was meshed into 152,859 isoparametric, and arbitrarily distorted tetrahedral elements connected by 26,090 nodes. The medium is firstly assumed to be homogeneous in elastic and magnetic properties in order to estimate separately the differences due to the topography.

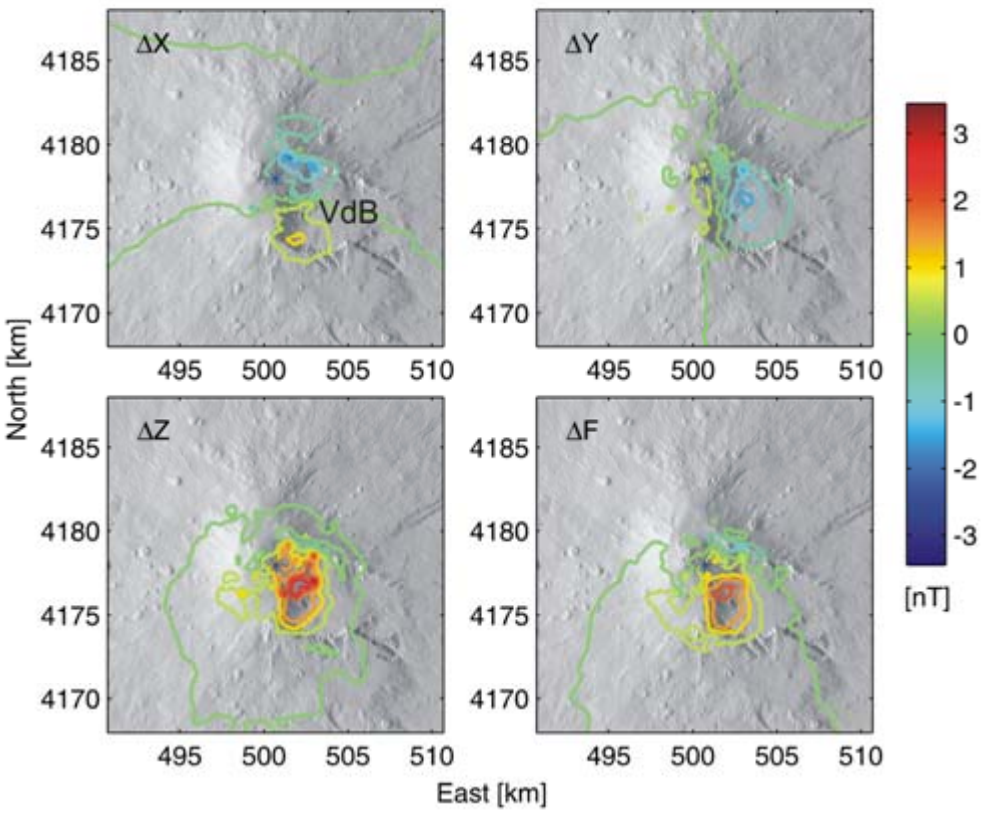

Magnetic field changes for a homogeneous magneto-elastic medium with the real topography of Mt Etna. Contour lines are at 0.5 nT. The star represents the pressure source location.

Effects of medium heterogeneity on piezomagnetic field

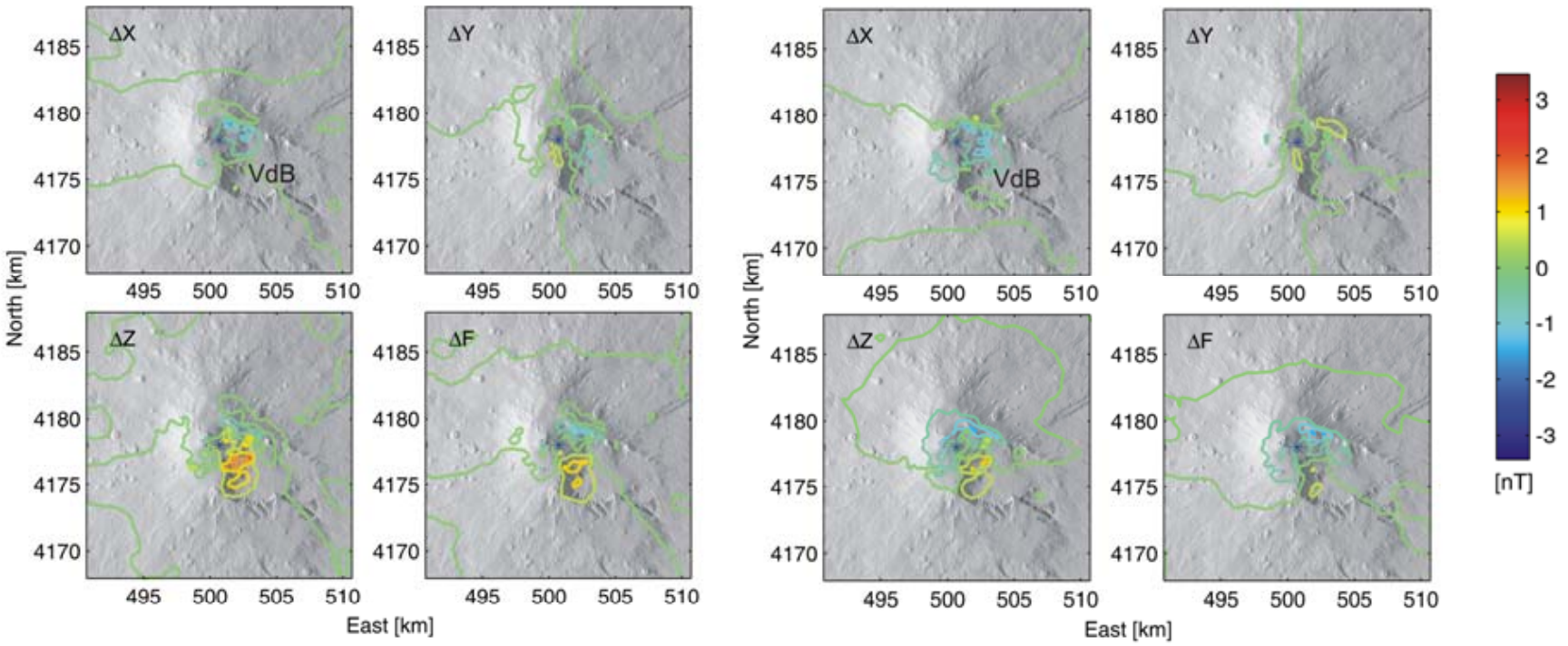

The magnetic field changes for a heterogeneous magneto-elastic medium (J_A on the left and J_B on the right) with the real topography of Mt Etna. The star represents the pressure source location.

Currenti et al., GJI 2009

Sezione di Catania

Etna 2008 Eruption

Istituto Nazionale di Geofisica e Vulcanologia

Seismic activity

(Domenico Patanè et al., INGV Report, 19 May 2008).

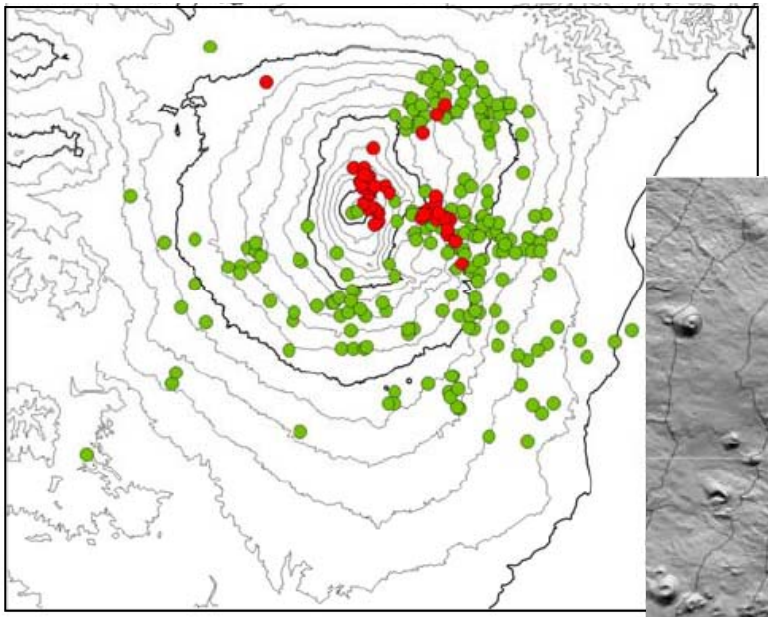

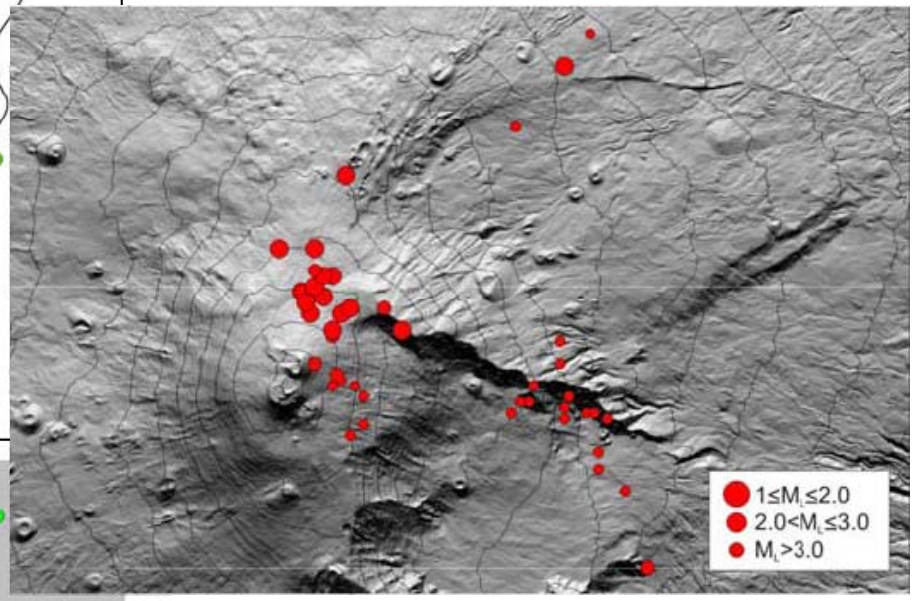

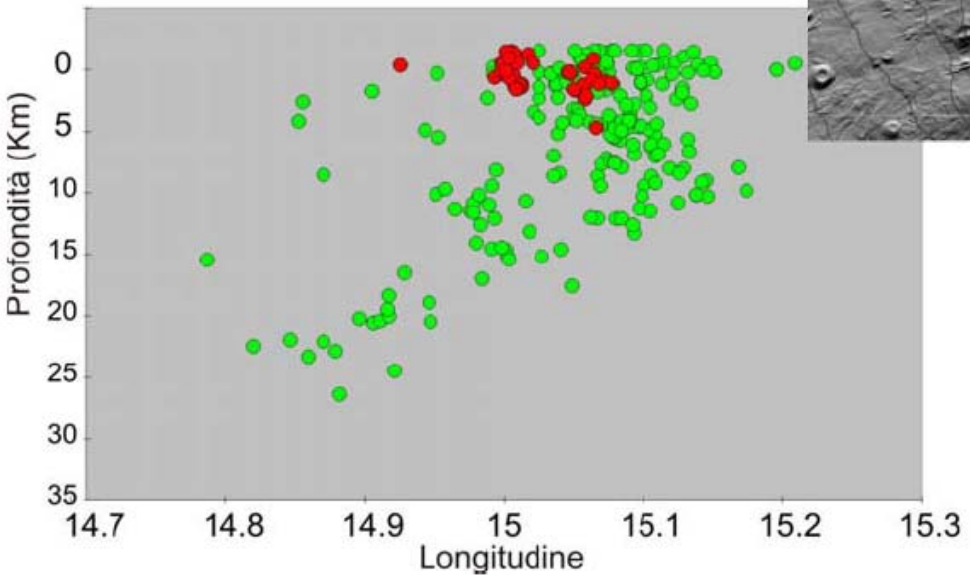

At left: Map of the epicenters and E-W cross-section of earthquakes occurred since January 2008 (in red earthquakes of 13th May). At right: map of the epicenters calculated on 13th May 2008.

Sezione di Catania

Istituto Nazionale di Geofisica e Vulcanologia

Fracture field

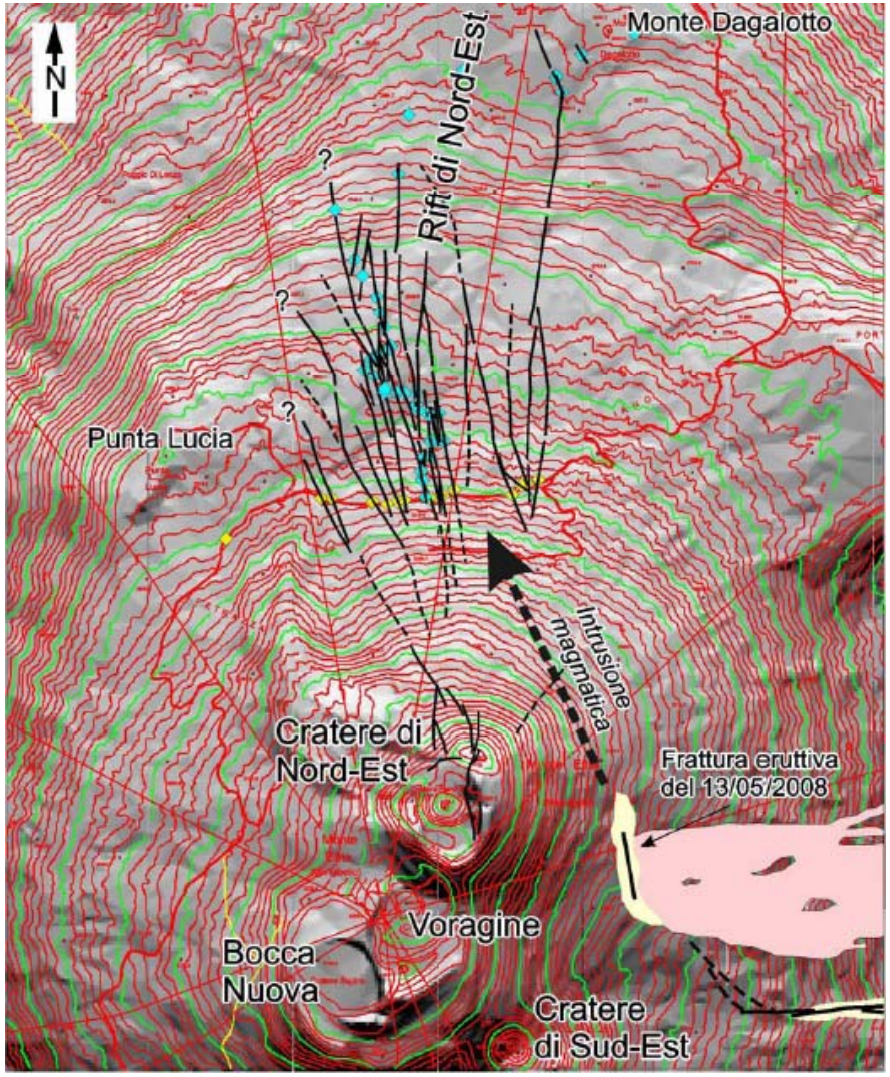

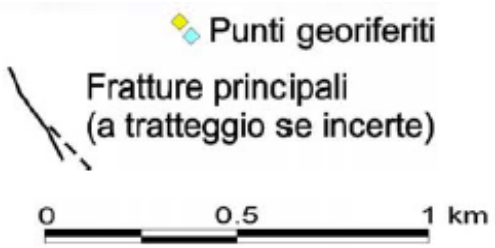

The fracture field, which remained dry extended from the base of the North-East crater for 2000 m along the NNW-SSE direction (Marco Neri, INGV Report, 22 May 2008).

Fracture Field

The N170E fracture field in the Northwestern flank of Etna (Gianni Lanzafame, INGV Report, 19 May 2008).

Geophysical Monitoring Data

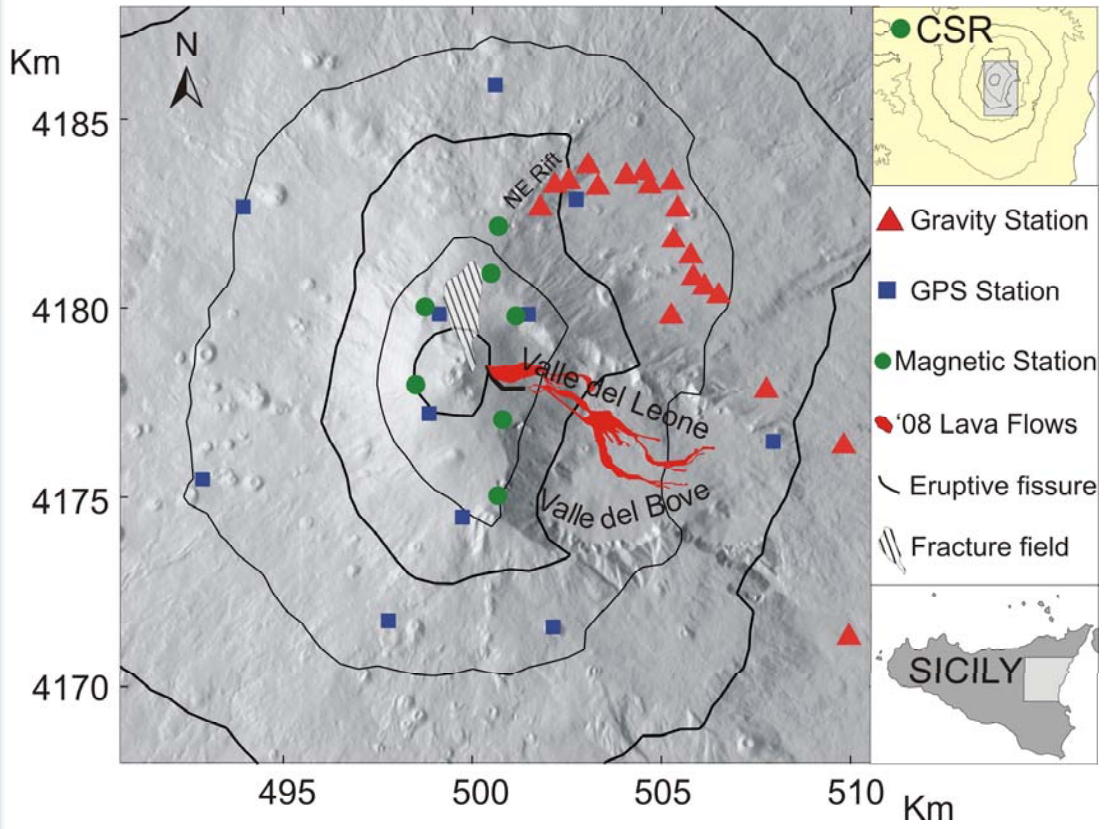

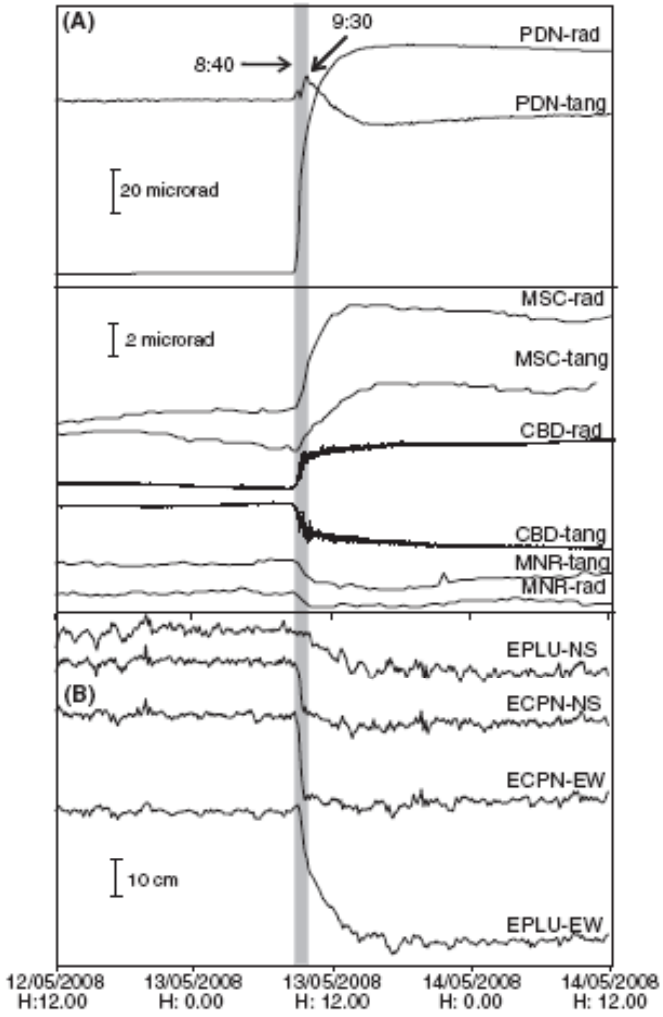

Radial and tangential tilt components recorded during the 13 May 2008 intrusion. Selected North–South (N–S) and East–West (E–W) components recorded by the GPS network.

Sezione di Catania

Istituto Nazionale di Geofisica e Vulcanologia

Daily mean differences of total intensity

A mobile daily averaging with an overlapping window of 2 hours is performed on magnetic data recorded in May to remove diurnal components.

No significant variations are observed before May 13th, while step-like variations at almost all stations are observed in time correspondence with the northward seismic swarm propagation.

The total magnetic field undergoes an irreversible change.

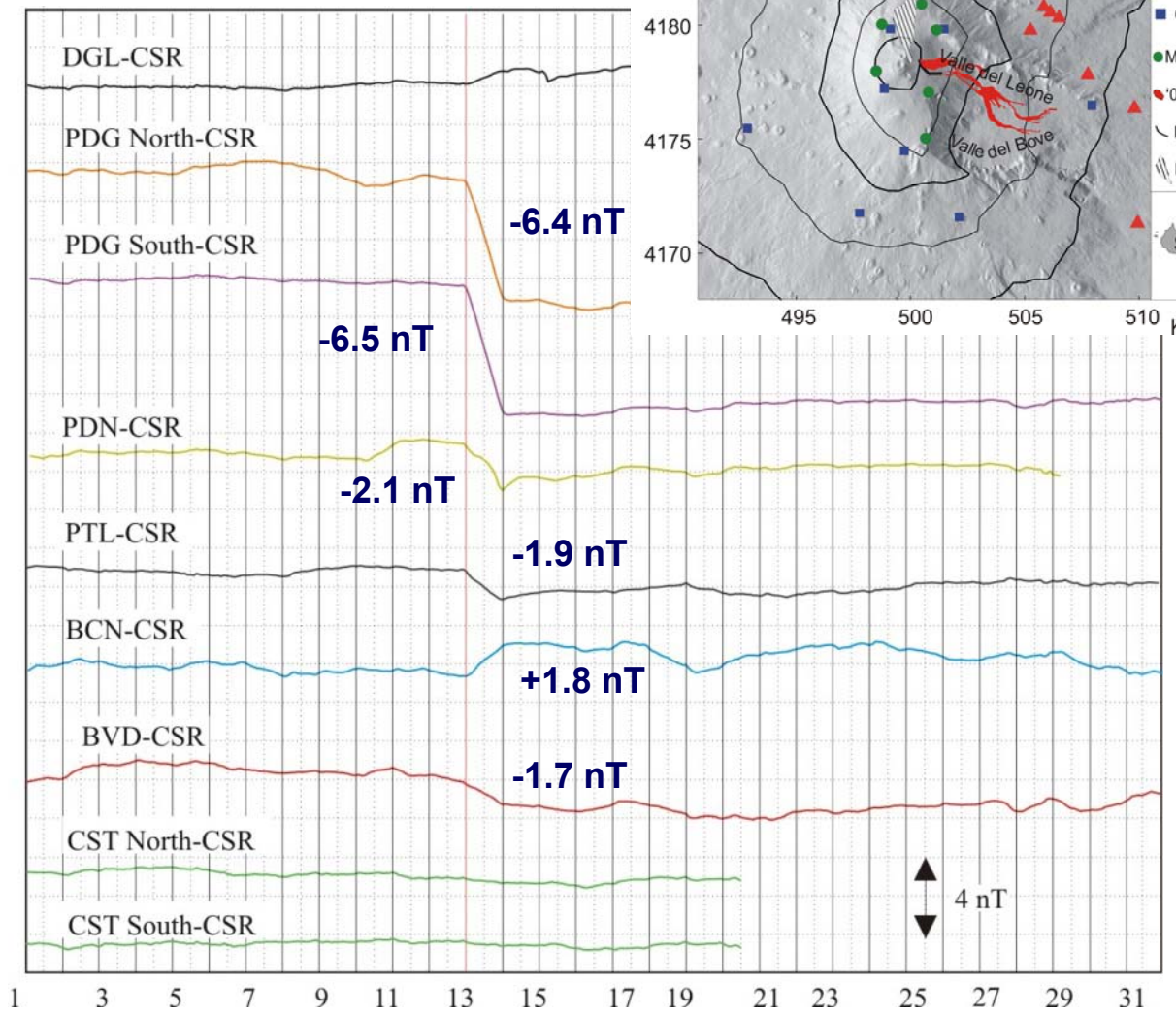

Sezione di Catania

Istituto Nazionale di Geofisica e Vulcanologia

10-minute means of total intensity

The magnetic data show a fast change from 09:00 to 10:00 GMT. In this time interval most of the earthquakes (about 150 of 230) were recorded.

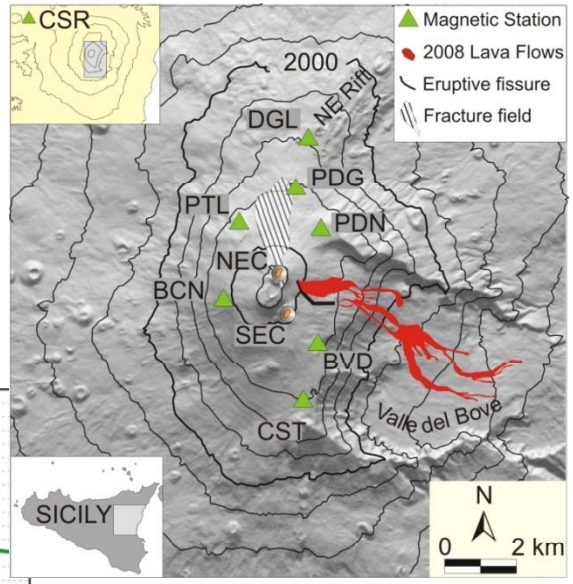

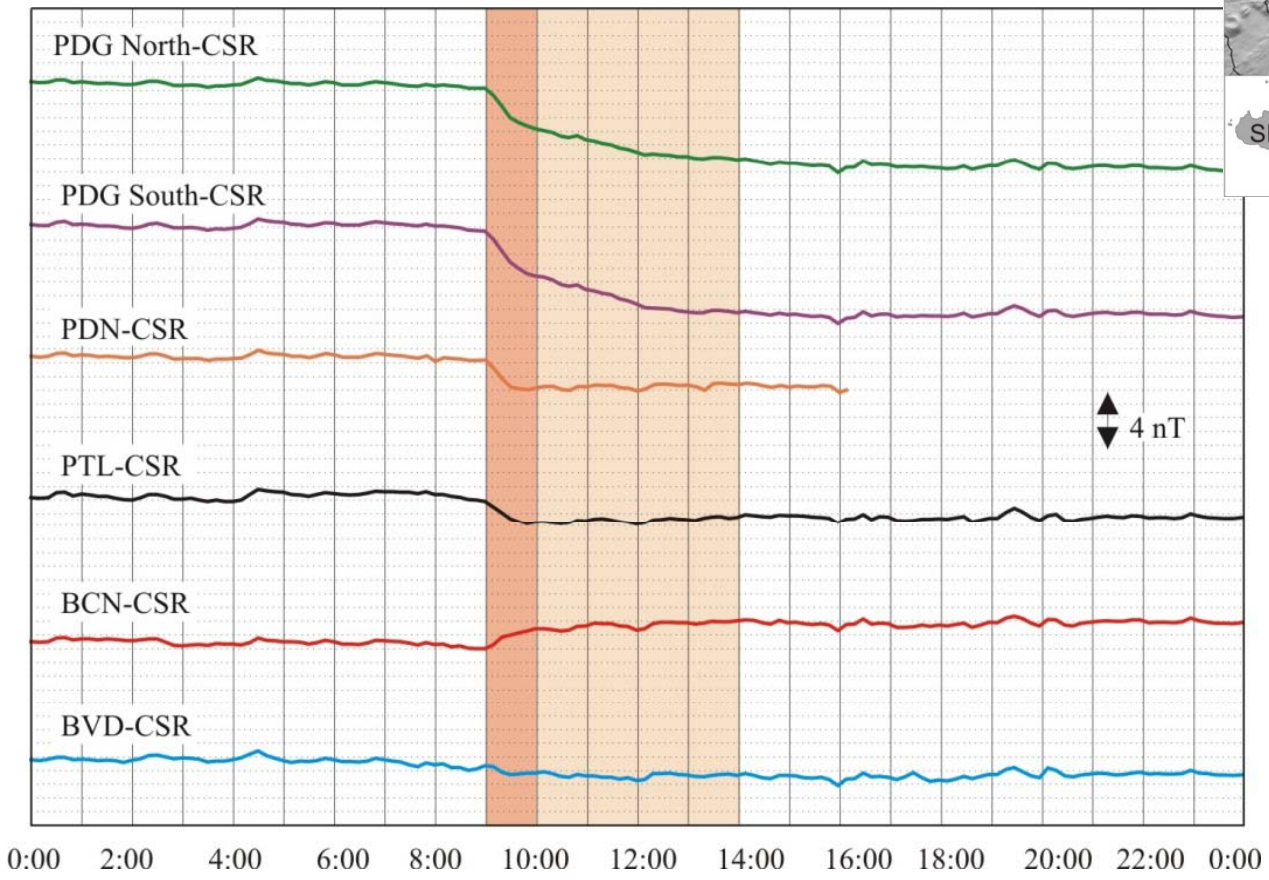

A decrease in the rate of magnetic variations was observed from 10:00 to 14:00 GMT during which a fall in the earthquake rate was observed. After the seismic swarm ended, no further magnetic variations were detected at all stations.

Sezione di Catania

Istituto Nazionale di Geofisica e Vulcanologia

Integrated Magnetic and Deformation Model

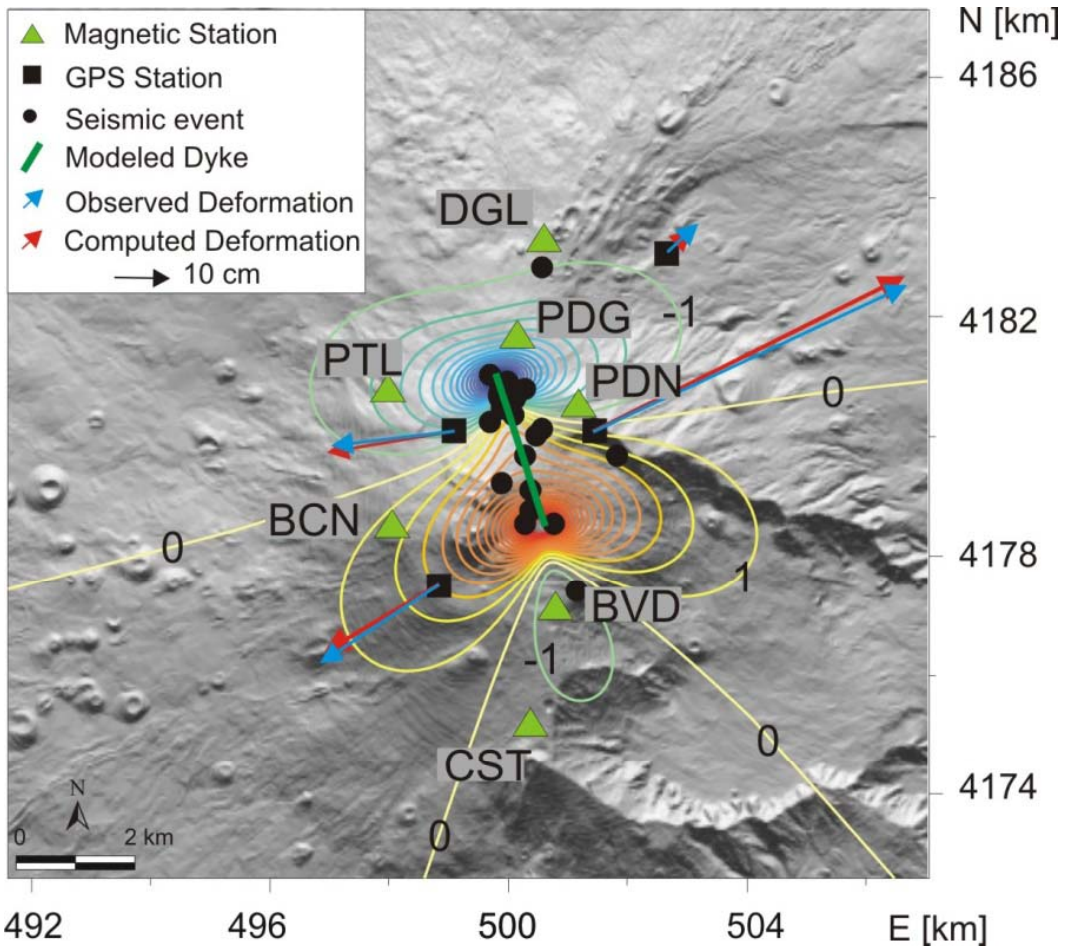

Magneto-elastic properties

Magnetization:	4 A/m
Inclination:	53.0°
Declination:	2°
Sensitivity:	10^{-4} bar^{-1}
Rigidity:	16 GPa

The estimated intrusive dike, which explains the observed magnetic data, engenders a deformation pattern [Okada, 1992] that well fits the ground deformation recorded by the continuous GPS network operating on Mt Etna.

Seismomagnetic signals: 1-minute mean differences

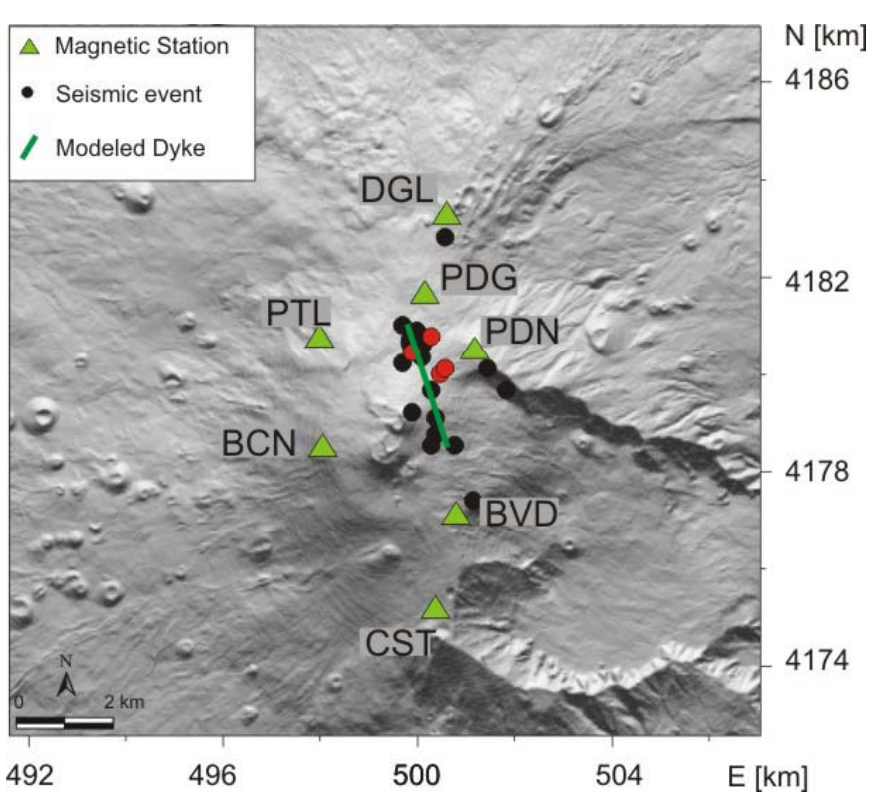

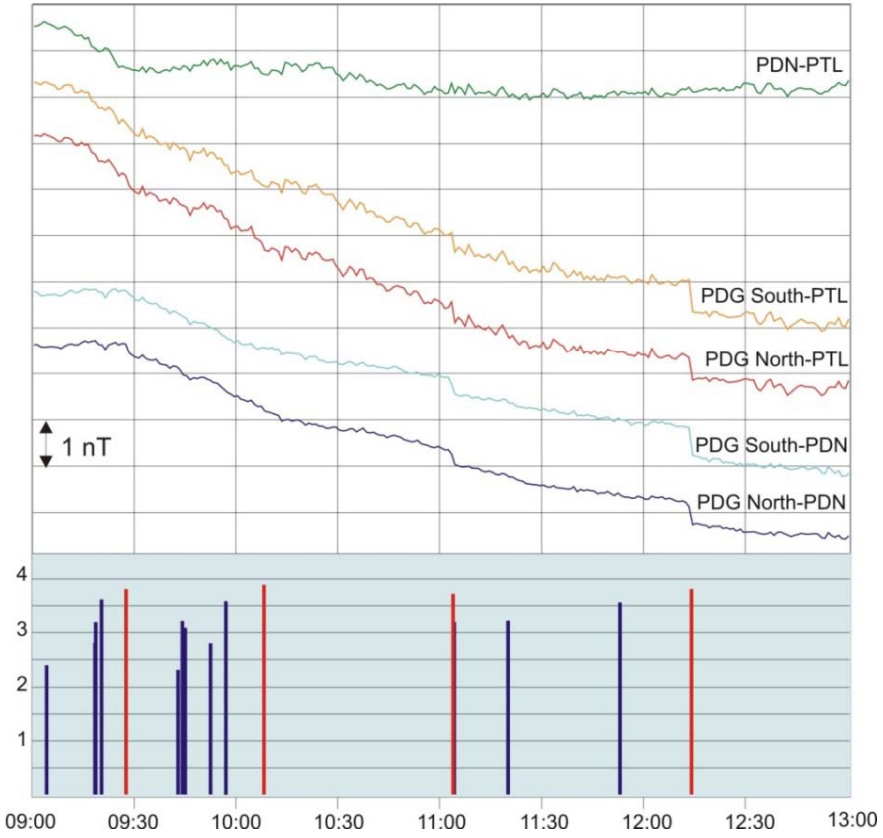

Rapid coseismic magnetic changes clearly identified on the northern flank in correspondence of 4 most energetic seismic events ($M_L \geq 3.5$). Step-like magnetic variations with amplitudes from 0.5 nT to 1 nT have been detected in the 1-minute mean differences of the magnetic signals.

Seismomagnetic signals at gradiometric stations

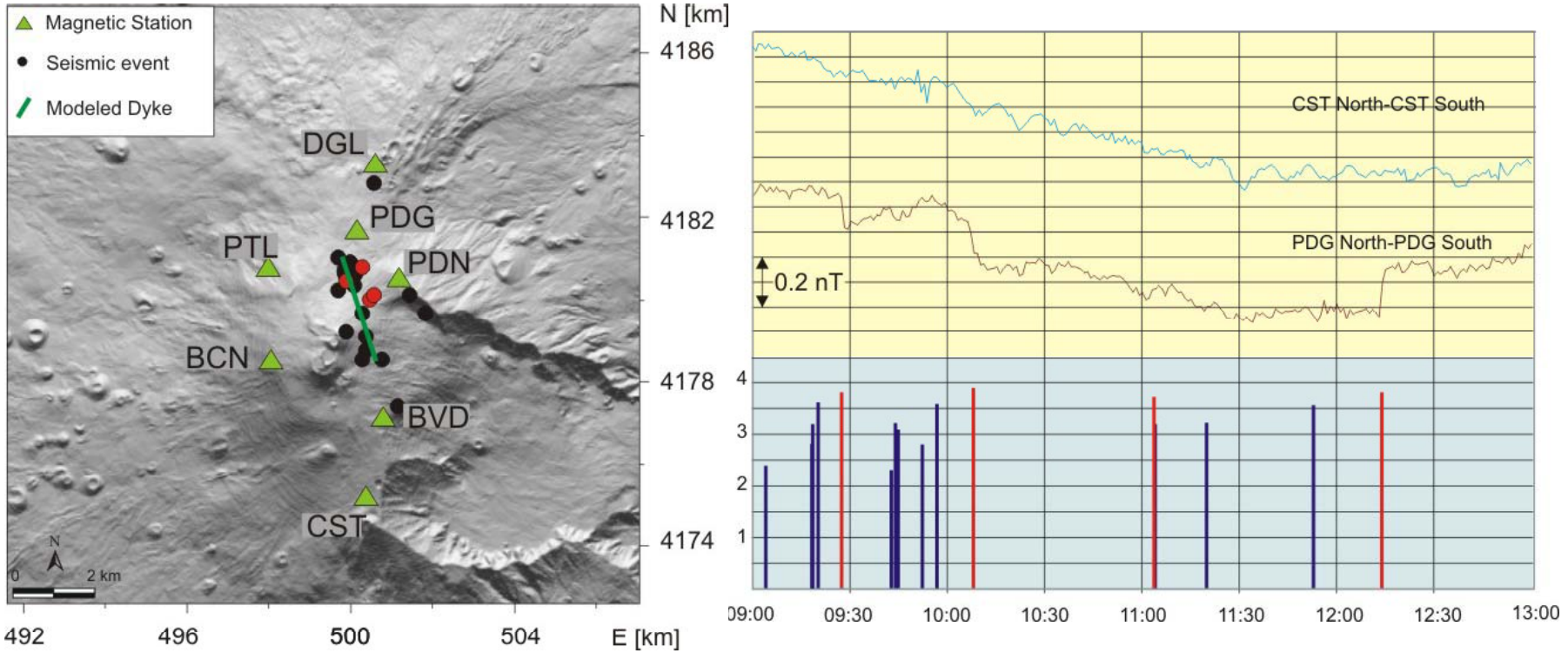

Significant rapid changes are clearly seen at PDG station, where the gradiometer configuration allows to discriminate sub-nanotesla variations thanks to the 50 m horizontal distance between the two sensors. The gradient at PDG shows magnetic offsets of about 0.3 nT in coincidence of the seismic events. No magnetic changes were, instead observed in the gradient field at CST located on the south flank.

Napoli et al., GRL 2008

Integrated Numerical Models: 2008 Etna eruption

The analytical model provided an acceptable representation of the magma intrusion, cannot explain all the details because a simple elastic half-space without topography and medium heterogeneity was used.

The horizontal deformation decrease because of the topography relief and the match with the observations improve. Instead, the piezomagnetic field changes show significant deviations from the homogeneous half-space solution. Significant discrepancies in shape and intensity are observed at most of the magnetic stations.

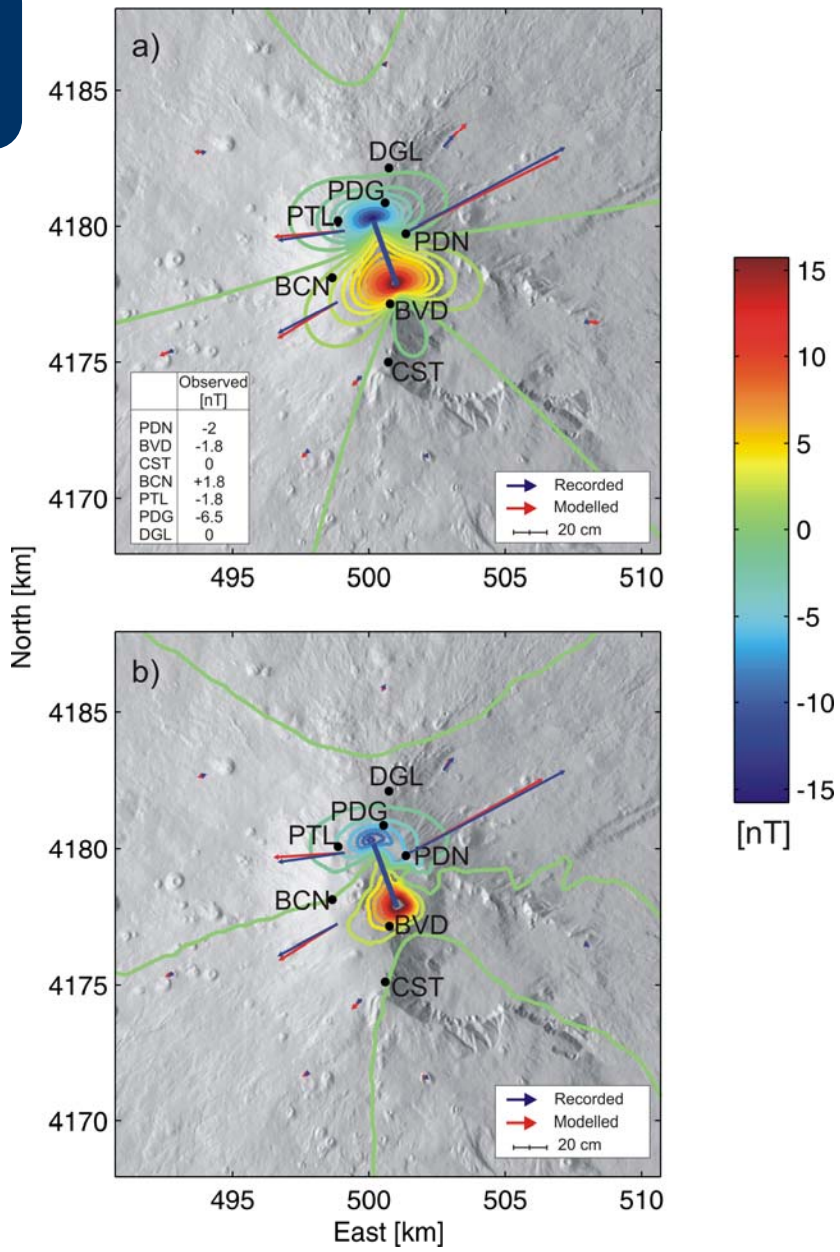

Sezione di Catania

Istituto Nazionale di Geofisica e Vulcanologia

Analytical Gravity Changes

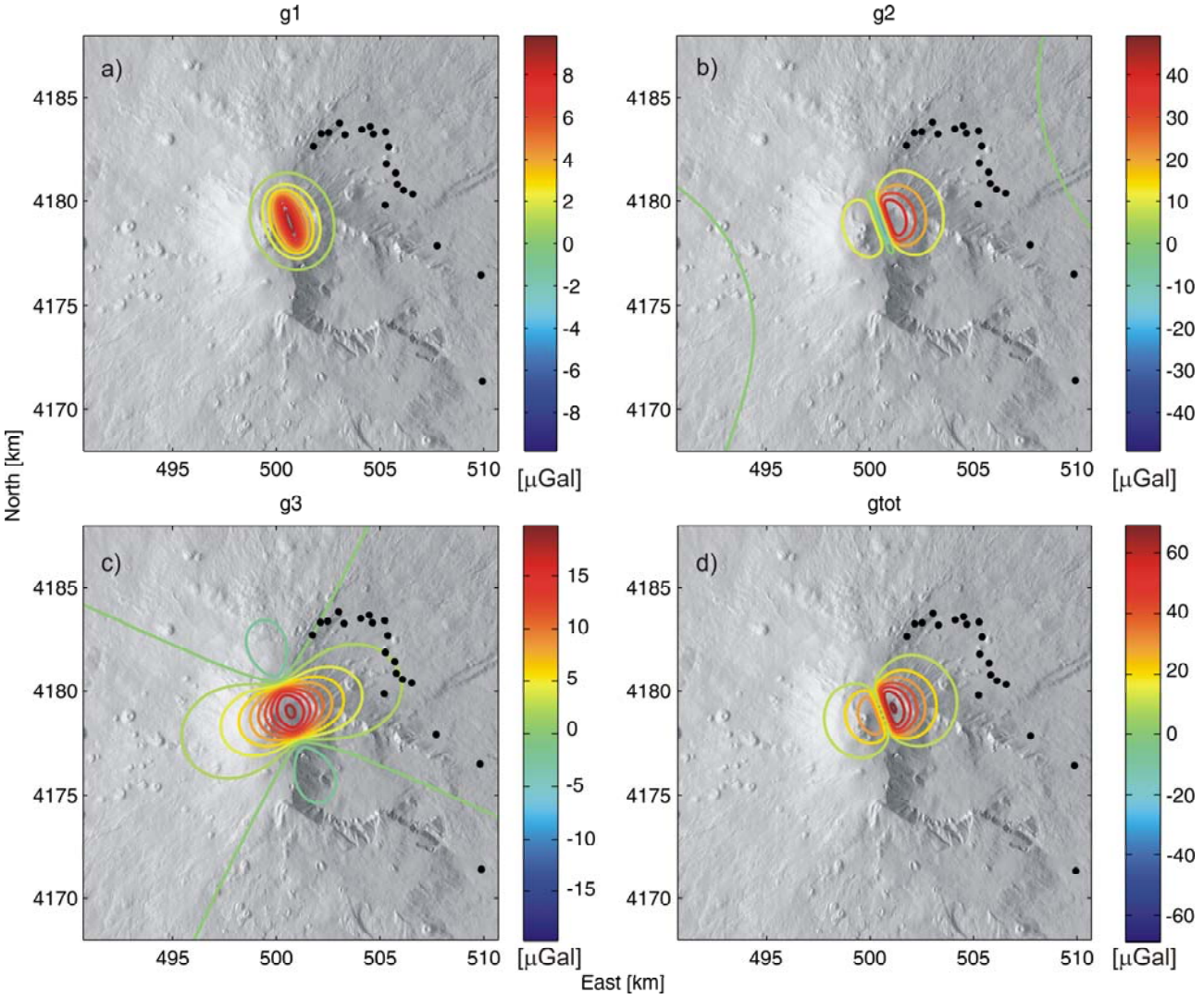

Sezione di Catania

Istituto Nazionale di Geofisica e Vulcanologia

Numerical Gravity Changes

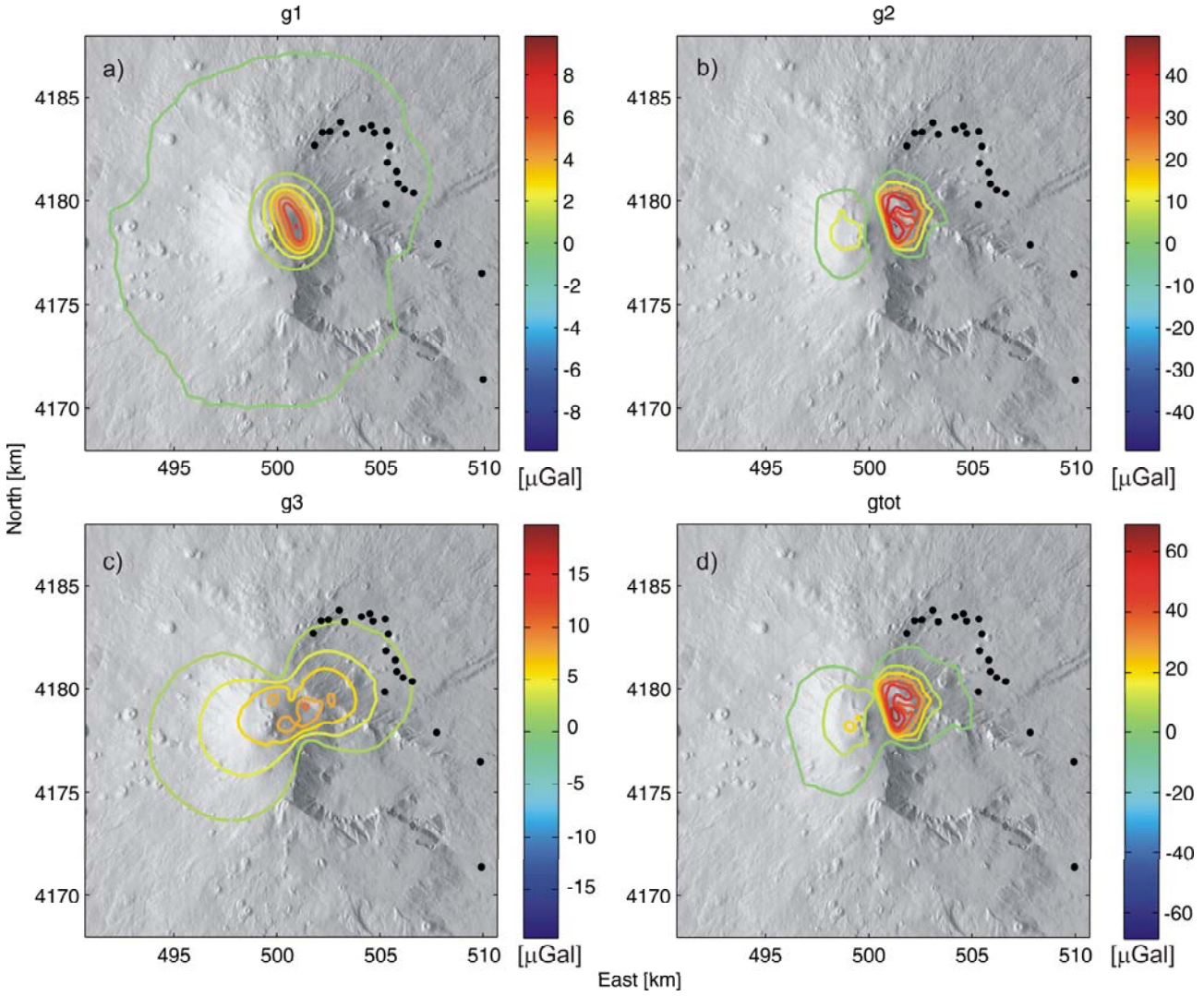

Sezione di Catania

Istituto Nazionale di Geofisica e Vulcanologia

Integrated Numerical Model

The match between the observed and the computed magnetic changes is improved at most stations. In particular, the computed piezomagnetic anomalies at BVD and PDN decrease in amplitude better fitting the magnetic observations. No significant differences are obtained at BCN.

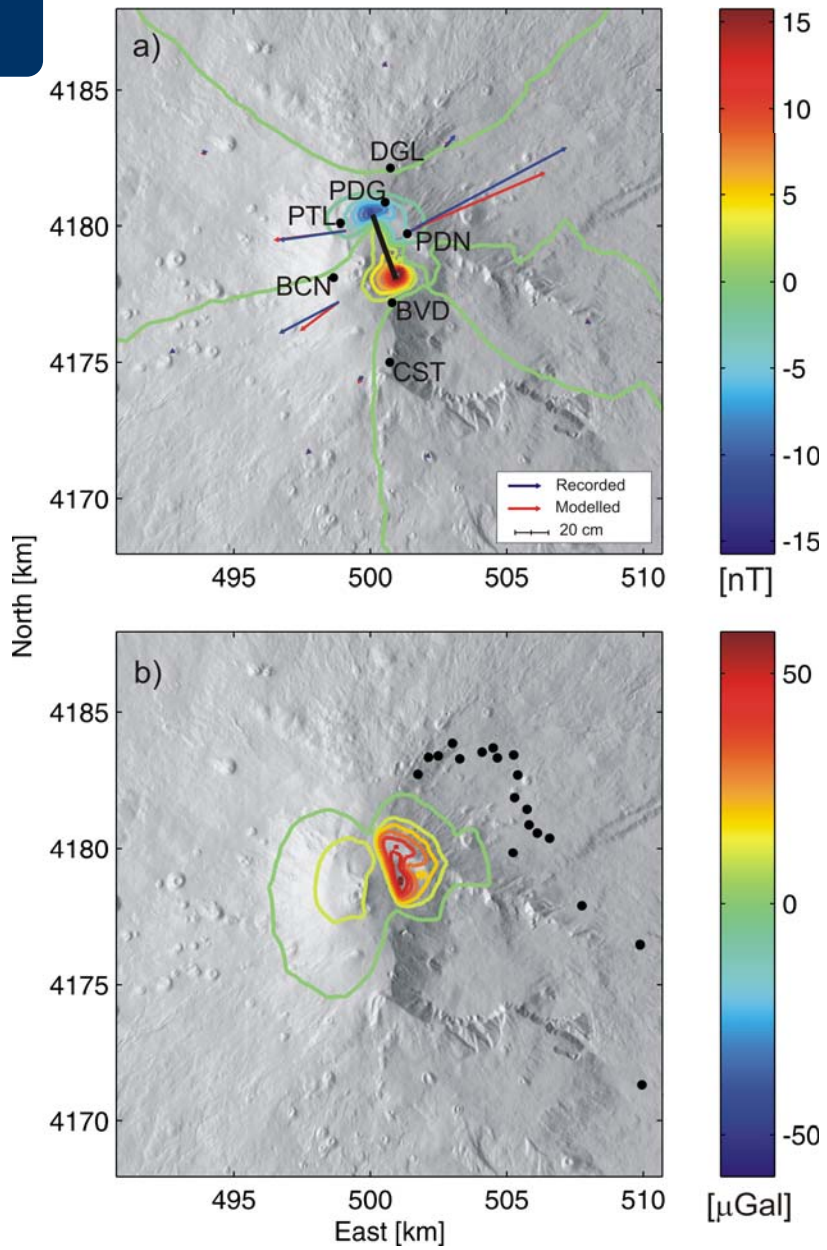

Conclusions

- Magnetic data allow to describe the most likely scenario occurred during the 2002-2003 and 2008 eruption

- Near real time magnetic data prove to be a key tool to update the state of the volcanic activity

- Integrated models of deformation and magnetic data allows to constraint the magmatic intrusion

- Rapid coseismic magnetic changes were identified in correspondence of most energetic seismic events ($M_L \geq 3.5$)

- Numerical model can enhance the reliability of model-based assessments of magnetic observations